1982

The effect of design parameters on shellside properties of baffled shell-and-tube heat exchangers.

Eden, Michael Spencer.

THE EFFECT OF DESIGN PARAMETERS ON SHELL-SIDE PROPERTIES OF BAFFLED SHELL-AND-TUBE HEAT EXCHANGERS

by

MICHAEL SPENCER EDEN
B.S., Miami University
Oxford, Ohio 1971

SUBMITTED IN PARTIAL FULFILLMENT OF THE REQUIREMENTS FOR THE DEGREES OF OCEAN ENGINEER AND MASTER OF SCIENCE IN NAVAL ARCHITECTURE AND MARINE ENGINEERING

at the

MASSACHUSETTS INSTITUTE OF TECHNOLOGY
May 1982

THE EFFECT OF DESIGN PARAMETERS ON SHELL-SIDE PROPERTIES OF BAFFLED SHELL-AND-TUBE HEAT EXCHANGERS

by

Michael Spencer Eden

Submitted to the Department of Ocean Engineering on May 7, 1982, in partial fulfillment of the requirements for the degrees of Ocean Engineer and Master of Science in Naval Architecture and Marine Engineering.

ABSTRACT

The Delaware Method of rating baffled shell and tube heat exchangers is used as the basis for a simplified mathematical model for predicting shell side heat transfer coefficients and pressure drops. Multiple non-linear regression analysis is used to express the heat transfer coefficient and pressure drop as a product of terms involving the five basic geometric parameters of a shell-and-tube heat exchanger, over a suitable range of these variables.

A brief sensitivity analysis of heat transfer per unit pressure drop is presented, along with a proposed routine for determining exchanger size when the shell-side coefficient is the controlling factor. A comparison is made between this method and the Delaware Method.

Thesis Supervisor: Warren M. Rohsenow
Title: Professor of Mechanical Engineering

ACKNOWLEDGMENTS

To my loving wife and son, an expression of thank you that words cannot convey, for three years of support and understanding.

To Professor Rohsenow, a most grateful appreciation for suggesting this thesis topic, for patience during my uncertain moments and for guidance in helping me "see the light at the end of the tunnel".

TABLE OF CONTENTS

NOMENCLATURE

A_i	heat transfer area for tube side, (ft^2)
A_o	heat transfer area for shell side, (ft^2)
c_s	specific heat of shell side fluid, (Btu/lbm - ^oF)
D_i	shell inside diameter, (in)
$D_{ot\ell}$	diameter of outer limit of tube bundle, (in)
d_o	tube outside diameter, (in)
d_i	tube inside diameter, (in)
F_c	fraction of tubes that are in crossflow
F_{sbp}	fraction of total crossflow area, available for bypass flow around tube bundle
f_i	gravitational friction factor for flow across an ideal tube bank
g_c	gravitational conversion constant, 4.17×10^8 lbm-ft/lbf-hr^2
h_i	tube side heat transfer coefficient (Btu/hr-ft^2-^oF)
h_{ideal}	ideal shell side heat transfer coefficient, (Btu/hr-ft^2-^oF)
h_o	exchanger shell side heat transfer coefficient, (Btu/hr-ft^2-^oF)

J_b	shell side heat transfer coefficient correction factor for bundle bypass effects
J_c	shell side heat transfer coefficient correction factor for baffle configuration effects
J_ℓ	shell side heat transfer coefficient correction factor for baffle leakage effects
J_r	shell side heat transfer coefficient correction factor for adverse temperature gradients
J_s	shell side heat transfer coefficient correction factor for the effect of unequal baffle spacing
j_i	Colburn j-factor for ideal tube bank
K_b	thermal conductivity of tube side fluid, (Btu/hr-ft-^{o}F)
K_s	thermal conductivity of shell side fluid, (Btu/hr-ft-^{o}F)
K_w	thermal conductivity of tube wall, (Btu/hr-ft-^{o}F)
$\Delta T_{\ell m}$	logarithmic mean temperature difference
L	effective tube length between tube sheets, (ft)
ℓ_c	baffle cut distance from baffle to shell inside diameter, (in)
ℓ_s	baffle spacing, (in)

$\ell_{s,i}, \ell_{s,o}$	baffle spacing at inlet and outlet of exchanger, respectively
N_b	number of baffles in exchanger
N_c	number of tube rows crossed during flow through one crossflow section
N_{cw}	number of effective crossflow rows in each window section
N_t	total number of tubes in exchanger
$\Delta P_{b,i}$	pressure drop for flow across one ideal crossflow section, (lbf/in^2)
$\Delta P_{w,i}$	pressure drop for flow through one ideal window section, (lbf/in^2)
p	tube pitch, (in)
p_n	tube pitch normal to flow, (in)
p_p	tube pitch parallel to flow, (in)
Q'	total heat transferred in heat exchanger, (Btu/hr)
R_b	pressure drop correction factor for effect of bundle bypass
R_ℓ	pressure drop correction factor for effect of baffle leakage
R_s	pressure drop correction factor for effect of unequal inlet and outlet baffle spacing

R_{e_s}	shell side Reynolds number
S_m	crossflow area at centerline for one crossflow section, (in^2)
S_{sb}	shell-to-baffle leakage area for one baffle, (in^2)
S_{tb}	tube-to-baffle leakage area for one baffle, (in^2)
S_w	area for flow through window, (in^2)
S_{wg}	total baffle window area, (in^2)
S_{wt}	window area occupied by tubes, (in^2)
U_o	overall heat transfer coefficient base on shell side heat transfer area, $(Btu/hr\text{-}ft^2\text{-}^oF)$
W_s	mass flow rate of shell side fluid, (lbm/hr)
W_t	mass flow rate of tube side fluid, (lbm/hr)
δ_{sb}	diametral clearance between shell and baffle, (in)
δ_{tb}	diametral clearance between tube and baffle, (in)
$\delta_{st\ell}$	approximate diametral clearance between shell and outer tube limit, (in)
μ_s	shell side fluid viscosity at bulk temperature, (lbm/hr-ft)

$\mu_{s,w}$	shell side fluid viscosity at surface temperature, (lbm/hr-ft)
ρ_s	shell side fluid density, (lbm/ft^3)
θ	baffle cut angle, (rad)
P_{r_s}	shell side Prandtl number
μ_b	tube side fluid viscosity at bulk temperature, (lbm/hr-ft)

LIST OF FIGURES

I. INTRODUCTION

A. BACKGROUND

The aim of any heat exchanger rating method is to predict, as accurately as possible, the performance of a heat exchanger with respect to total heat transferred and pressure drops encountered on both the shell and tube sides.

The Delaware Method for Rating Baffled Shell and Tube Heat Exchangers (1) was developed from its inception in the late 1940's through the early 1960's as a result of numerous experiments conducted at the University of Delaware. This method is applicable to many variations on the baffled exchanger: multiple passes, finned tubes, various tube orientations, a wide range of Reynolds numbers, etc. As Bell has stated (1), the method does have its uncertainties, as all methods do. However, this method is widely used and easy to understand.

Tinker (2) and Devore (3) propose similar methods for rating baffled exchangers, but, in the opinion of this author, are not as straightforward as the Delaware Method. Bell himself has proposed routines for sizing baffled exchangers based on the Delaware Method (references 1 and 11), and this method has been used extensively in computer programs for "optimal" exchanger determination. References (9) and (10) are two such examples.

The basic means of analysis in the Delaware Method takes into consideration five fluid streams and three heat transfer zones in the baffled exchanger, as illustrated in Figures 1 and 2. As can be seen by these simplified illustrations, the flow pattern for shell side fluid is complex at best. Reference (1) contains the complete set of equations for relating the heat transfer coefficient and pressure drops to the geometry of the exchanger. This reference also utilizes extensively graphs and tables for determination of some parameters. Mueller (7) has developed equations for many of these graphical relations. Appendix A is a compilation of the basic equations of the Delaware Method and those derived by Mueller. This compilation does have its limitations as noted in Section I.C.

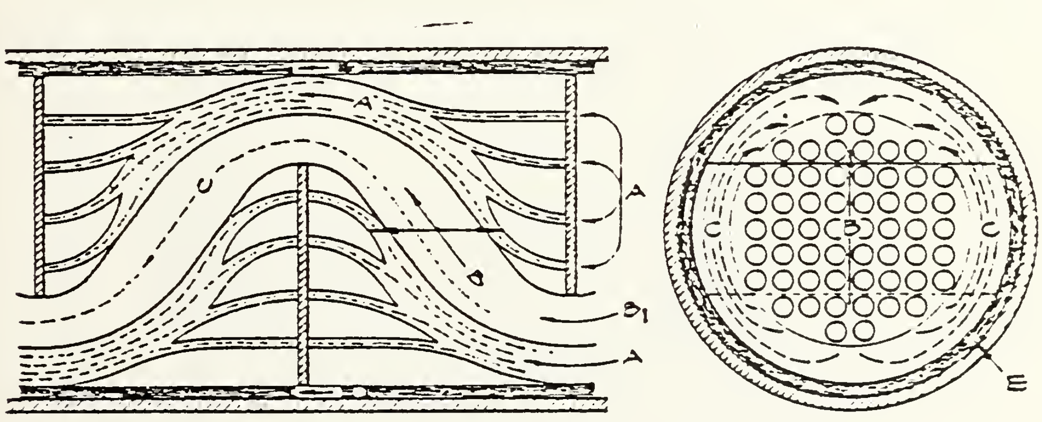

FIGURE 1 Schematic Diagram of Streams on Shell Side of Baffled Heat Exchangers.

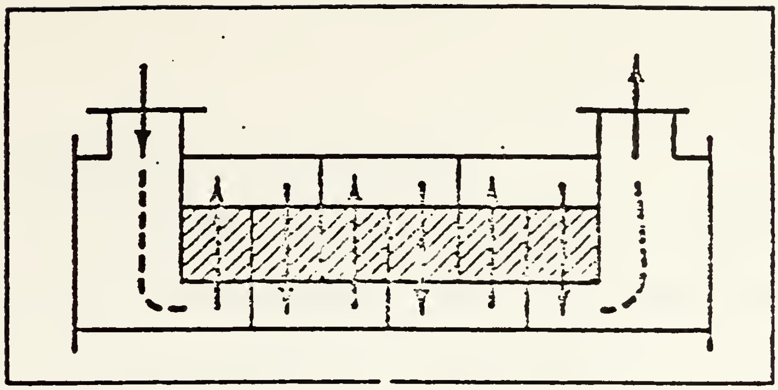

FIGURE 2(a) Region of Crossflow Between Baffle Tips in the Central Baffle Spacing

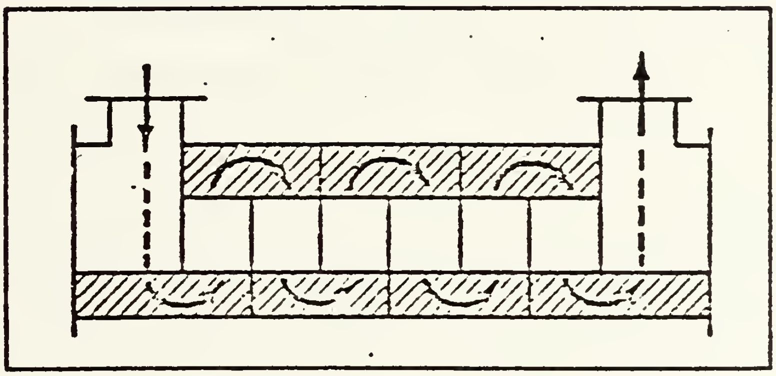

FIGURE 2(b) Flow Region Considered for Window Flow

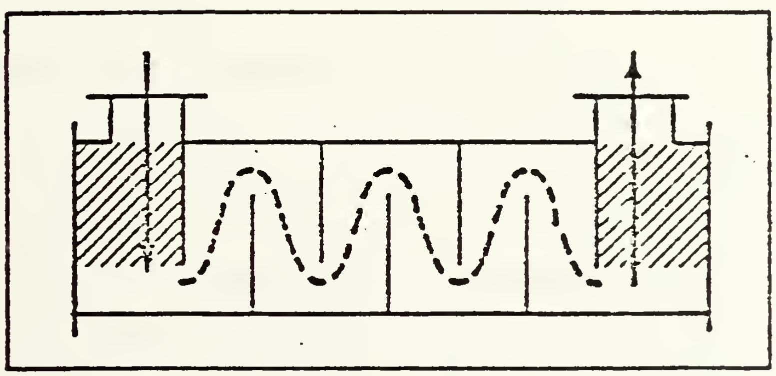

FIGURE 2(c) Flow Region for the End Baffle Spacings

B. PURPOSE AND METHODOLOGY

The purpose of this study is to provide an insight into the relations between shell-side heat transfer coefficient and pressure drop and the five basic exchanger parameters: Tube diameter -- d_o; pitch-to-diameter ratio -- P/d_o; baffle cut ratio -- ℓ_c/D_i; baffle spacing ratio -- ℓ_s/D_i; and shell diameter -- D_i.

It is anticipated that a simplified model for determining the heat transfer coefficient will be of considerable use to the designer as a "first cut" in sizing an exchanger for a given job. Admittedly, this cannot replace the sophisticated computer programs available for the determination of "optimal" exchanger configuration for a given application. However, the method developed here will be a step in the right direction for initial selection of parameters and will provide some "feel" for the effect of geometry variations on overall heat exchanger performance.

This analysis was conducted utilizing the basic equations of the Delaware Method as modified by the assumptions and approximations enumerated in Section I.C. Utilizing these equations, those factors affecting heat transfer and pressure drop which are a function of exchanger geometry were calculated over a suitable range

of variables. The resulting values were correlated utilizing four FORTRAN subroutines (b): CORRE, ORDER, MINV and MULTR. The resulting non-linear correlation yields these factors expressed as a product of the five basic exchanger parameters, each with its own regression coefficient as an exponent, and a single correlation coefficient. These regressions provided acceptable correlation results, the maximum overall error being on the order of five percent.

C. LIMITATIONS/ASSUMPTIONS/APPROXIMATIONS

1. Limitations

In this analysis, no attempt has been made to correlate data for the shell side heat transfer co-efficient where sealing strips are used to limit the bundle bypass flow. Nor has an attempt been made with regard to enhanced surfaces for heat transfer, i.e. finned tubes. Finally, only the single pass condition for the tube side fluid is taken into consideration. Admittedly, these restrictions limit the scope of this study with regard to overall applicability to heat exchanger design. However, it is hoped that this analysis will provide insight into the basic relations between shell side heat transfer coefficient and the fundamental exchanger goemetric parameters.

2. Assumptions

It is realized that manufacturing considerations effect significantly the design, construction and final form of any heat exchanger. Reference (5) sets standards for the tube-to-baffle and baffle-to-shell diametral clearances for various applications. These values are predominantly of the "step function" type, in that they can not be expressed as a continuous dependent variable based on any of the independent exchanger parameters. For the purposes of this study, both clearances were assumed constant throughout the range of parameters considered. The values used for these clearances are:

Shell-to-baffle clearance: δ_{sb} = 0.175 inches

Tube-to-baffle clearance: δ_{tb} = 0.03125 inches

These assumptions again allow concentration on the effect of major exchanger parameters.

The second major assumption is the neglect of unequal baffle spacing for inlet and outlet passages. This assumption is made in both heat transfer coefficient and pressure drop calculations. Unequal baffle spacing, in an exchanger where the ratios

$$\frac{\ell_{s,i}}{\ell_s} = \frac{\ell_{s,o}}{\ell_s} = 1.5,$$

contributes to an approximate 2-3% reduction in the overall heat transfer coefficient for a sufficiently large number of baffles. Where pressure drop is concerned, the assumption must be made with the realization that the end zones be considered as crossflow areas identical to the zones between the baffles. Equations (19) and (25) of Appendix A reflect these changes.

3. Approximations

In order to implement any numerical analysis of the type used in this study, it is necessary to derive relations from data provided by the manufacturing community and from curves of friction factor and Colburn j-factor.

For the former, references (1), (5) and (8) were used for two such derivations. The number of tubes in a heat exchanger of particular shell diameter was correlated as a function of shell inside diameter, pitch-to-tube diameter, and tube diameter, for the single-pass condition. These results are:

For square/rotated square tube layouts:

$$N_t = 0.3559 \frac{D_i^{2.17526}}{d_o^{\,2}} \left(\frac{d_o}{P}\right)^2 \qquad (1)$$

For triangular tube layouts:

$$N_t = 0.40759 \frac{D_i^{\,2.1797}}{d_o^{\,2}} \left(\frac{d_o}{P}\right)^2 \qquad (2)$$

These approximations give results within 5% over the range of shell diameters from 10 to 60 inches. The clearance for bundle bypass flow ($D_i - D_{ot\ell}$) was correlated as a function of shell diameter also, resulting in the approximation:

$$\delta_{st\ell} = (D_i - D_{ot\ell}) = 0.5817\, D_i^{\,0.3066} \qquad (3)$$

Figures 3, 4, and 5 are graphs of friction factor and Colburn j-factor versus shell-side Reynolds number for the various tube orientations at varying pitch-to-tube diameter ratios. Correlation results are presented in Tables 1 and 2 for friction factor and Colburn j-factor, respectively, for the separate ranges of Reynolds numbers shown.

Table 3 presents relations between tube pitch, tube pitch normal to fluid flow and tube pitch parallel to fluid flow for the various orientations. These relations are used in equations (1), (3), and (4) of Appendix A in calculating the various factors associated with heat transfer and pressure drop calculations.

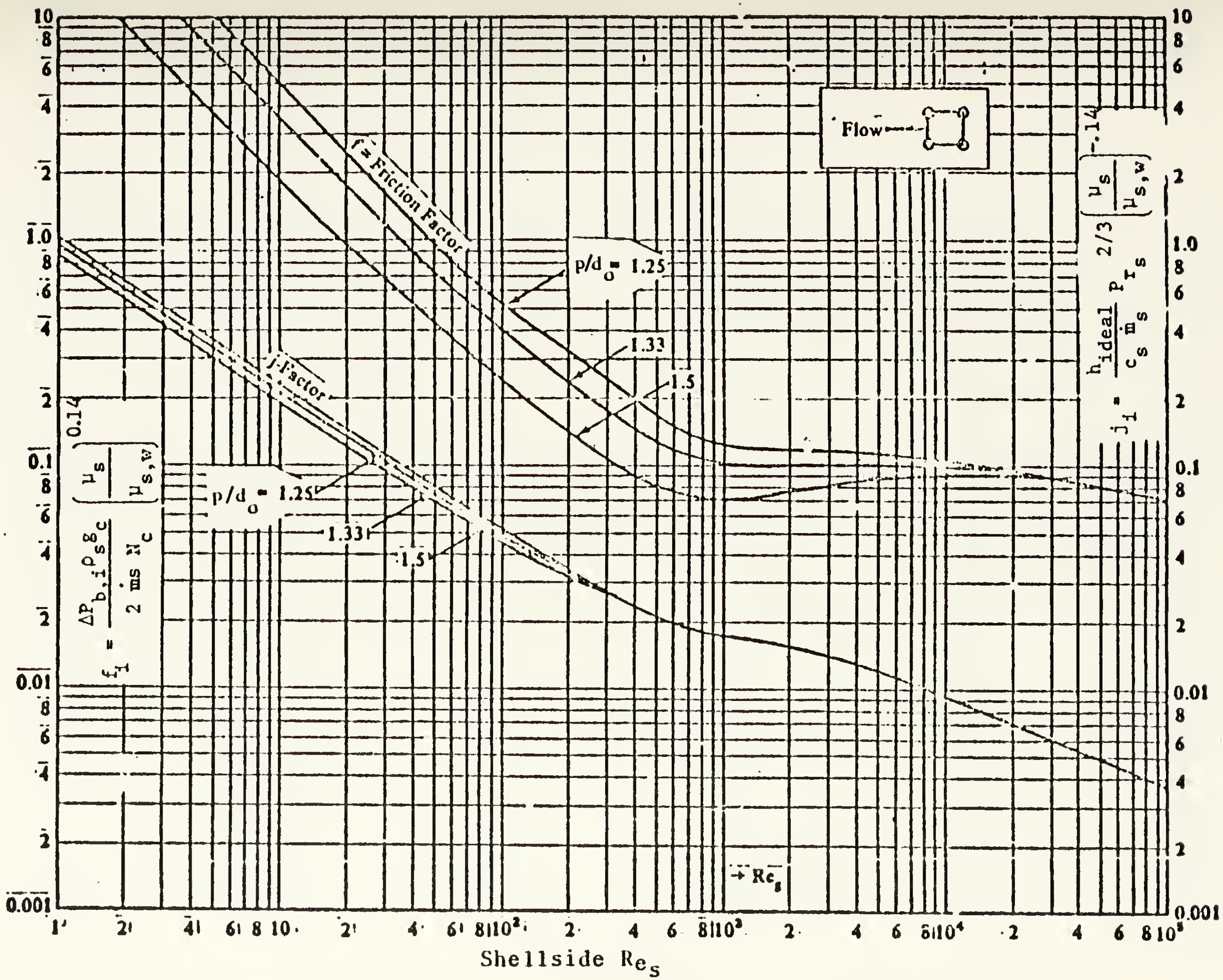

FIGURE 3 Ideal Tube Bank j_i and f_i Factors for 90° In-Line Layout

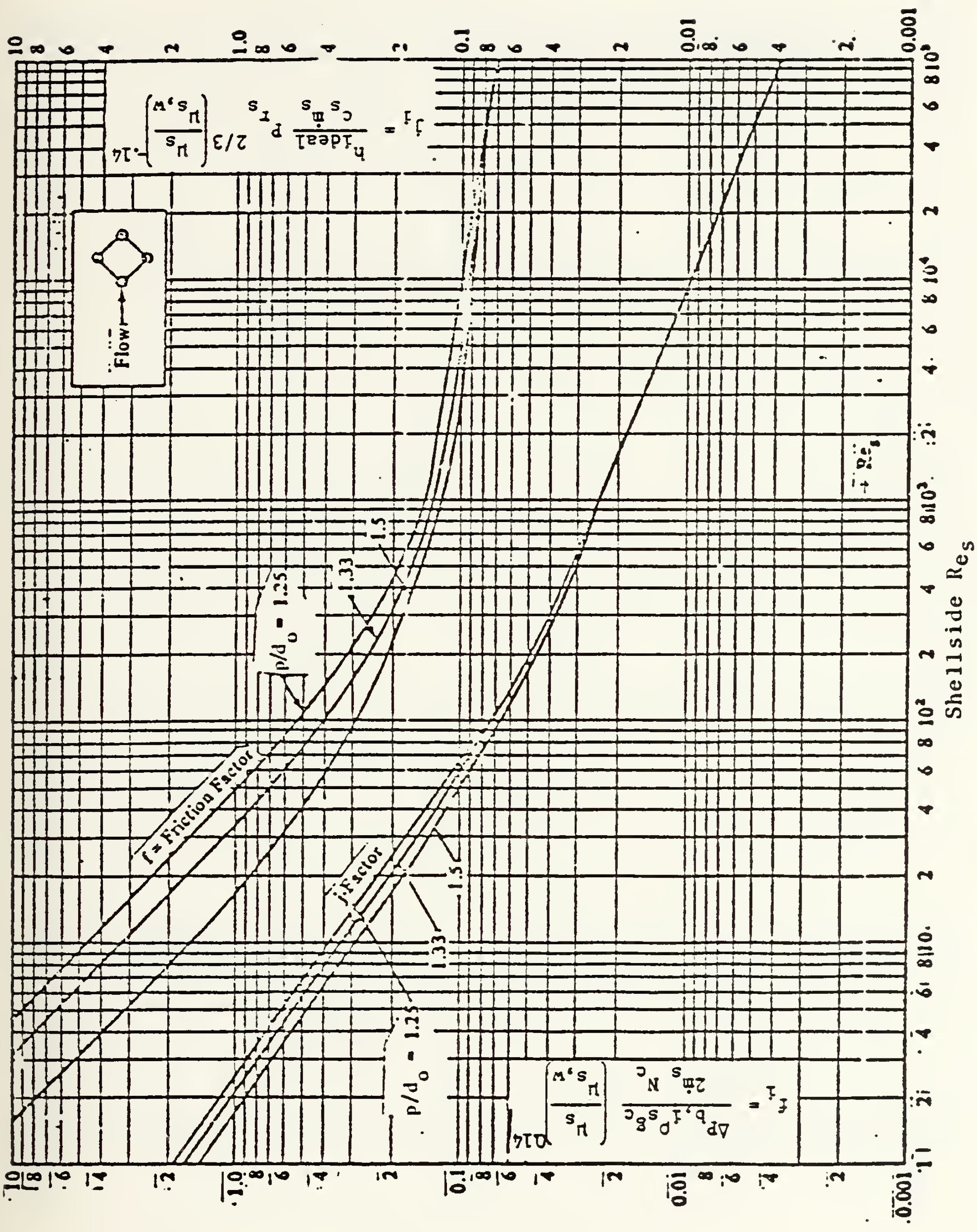

FIGURE 4 Ideal Tube Bank j_i and f_i Factors for 45^{o} Staggered Layout

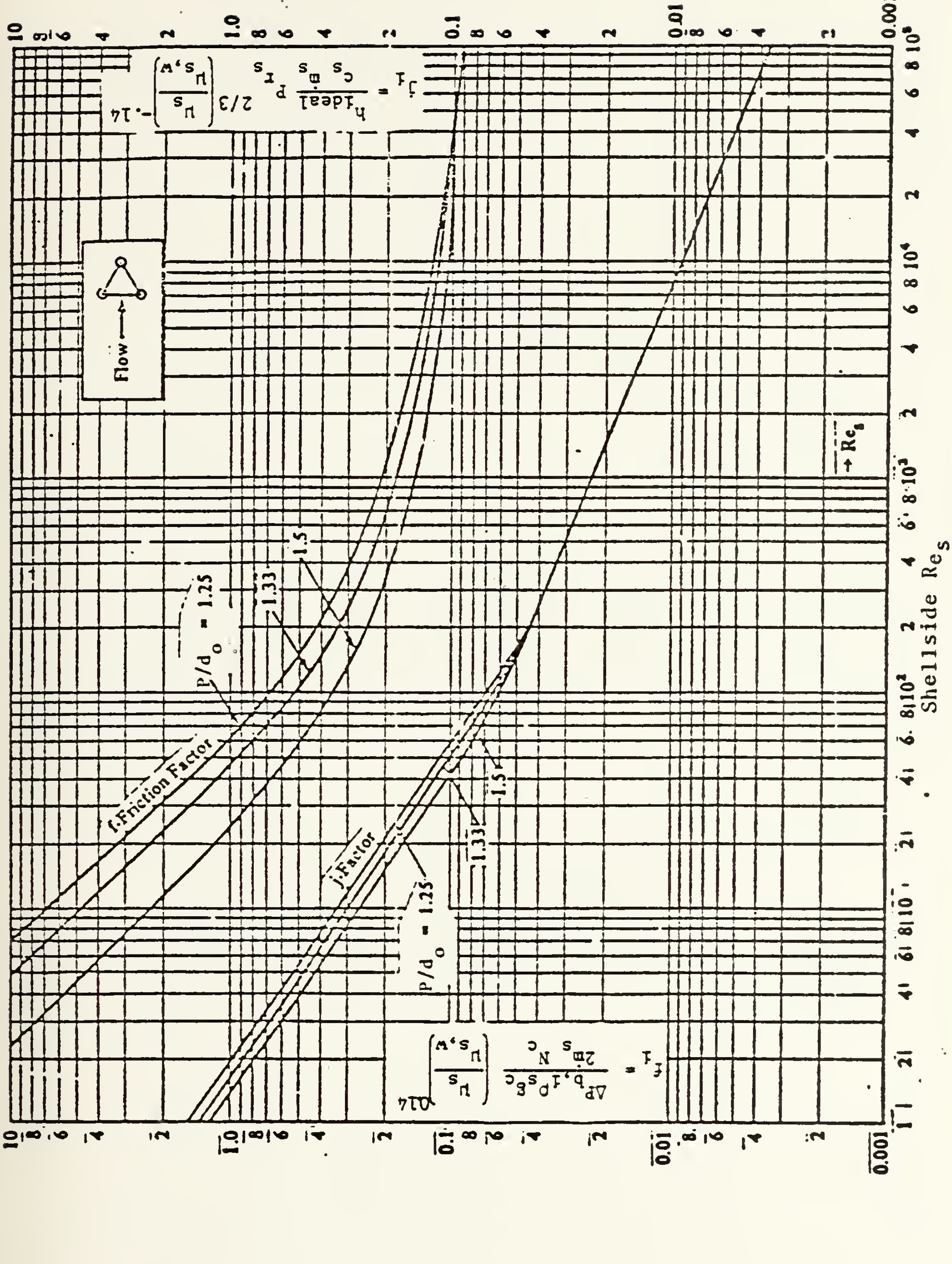

FIGURE 5 Ideal Tube Bank j_i and f_i Factors for 30^o Staggered Layout

$$j_i = a_o (R_{e_s})^{a_1} (P/d_o)^{a_2}$$

R_{e_s}	Layout	a_o	a_1	a_2
	square	1.0645	-0.598	-0.7203
$1 - 10^3$	rotated-square	1.9492	-0.6282	-0.9858
	triangular	1.6505	-0.6114	-0.8484
	square	0.2257	-0.3532	0
$10^3 - 10^5$	rotated-square	0.3773	-0.3976	0
	triangular	0.337	-0.3921	0

TABLE 1 j-Factor Correlation Results

$$f = f(R_{e_s}, P/d_o) = a_o (R_{e_s})^{a_1} (P/d_o)^{a_2}$$

R_{e_s}	Layout	a_o	a_1	a_2
$1 - 10^3$	square	80.29	-0.853	-4.183
	rotated square	51.1	-0.746	-3.918
	triangular	75.12	-0.747	-4.176
$10^3 - 10^5$	square	0.2565	-0.0664	-1.383
	rotated square	0.3561	-0.1276	-0.502
	triangular	0.4043	-0.1114	-0.749

TABLE 2 Friction Factor Correlation Results

P = tube pitch

P_n = tube pitch normal to flow

P_p = tube pitch parallel to flow

Tube Orientation	P_n	P_p
square	1.0 P	1.0 P
rotated square	$\sqrt{2}/2$ P	$\sqrt{2}/2$ P
triangular	P/2	$\sqrt{3}/2$ P

TABLE 3 Relations Between Tube Pitch P, and P_n, P_p for Various Tube Orientations

D. NEGLECTED FACTORS J_r and J_s

For preliminary estimation and sizing as proposed by this simplification, the factors J_r (correction due to adverse temperature gradients) and J_s (correction due to unequal inlet and outlet baffle spacing) have been neglected.

To account for the effect of J_s, the final heat exchanger length must be known, which allows determination of the end baffle spacing. J_s may then be calculated from:

$$J_s = \frac{(N_{b-1}) + \ell_{s,i}^{*\,(.4)} + \ell_{s,o}^{*\,(.4)}}{(N_{b-1}) + \ell_{s,i}^{*} + \ell_{s,o}^{*}} \tag{4}$$

where

$$\ell_{s,i}^{*} = \ell_{s,i}/\ell_s, \quad \ell_{s,o}^{*} = \ell_{s,o}/\ell_s$$

The initial value of h_o must then be multiplied by J_s to give a more accurate estimate.

The factor J_r is calculated only in laminar flow ($R_{e_s} < 100$) from:

$$J_r = \frac{1.51}{(N_c)} 0.18 \tag{5}$$

Should this condition ($R_{e_s} < 100$) exist, again adjust h_o by multiplying by J_r. Figures 6 and 7 show graphically the relations for J_s vs $\ell^*_{s,i}$ and J_r vs N_c. These graphs may be used in lieu of actual calculations.

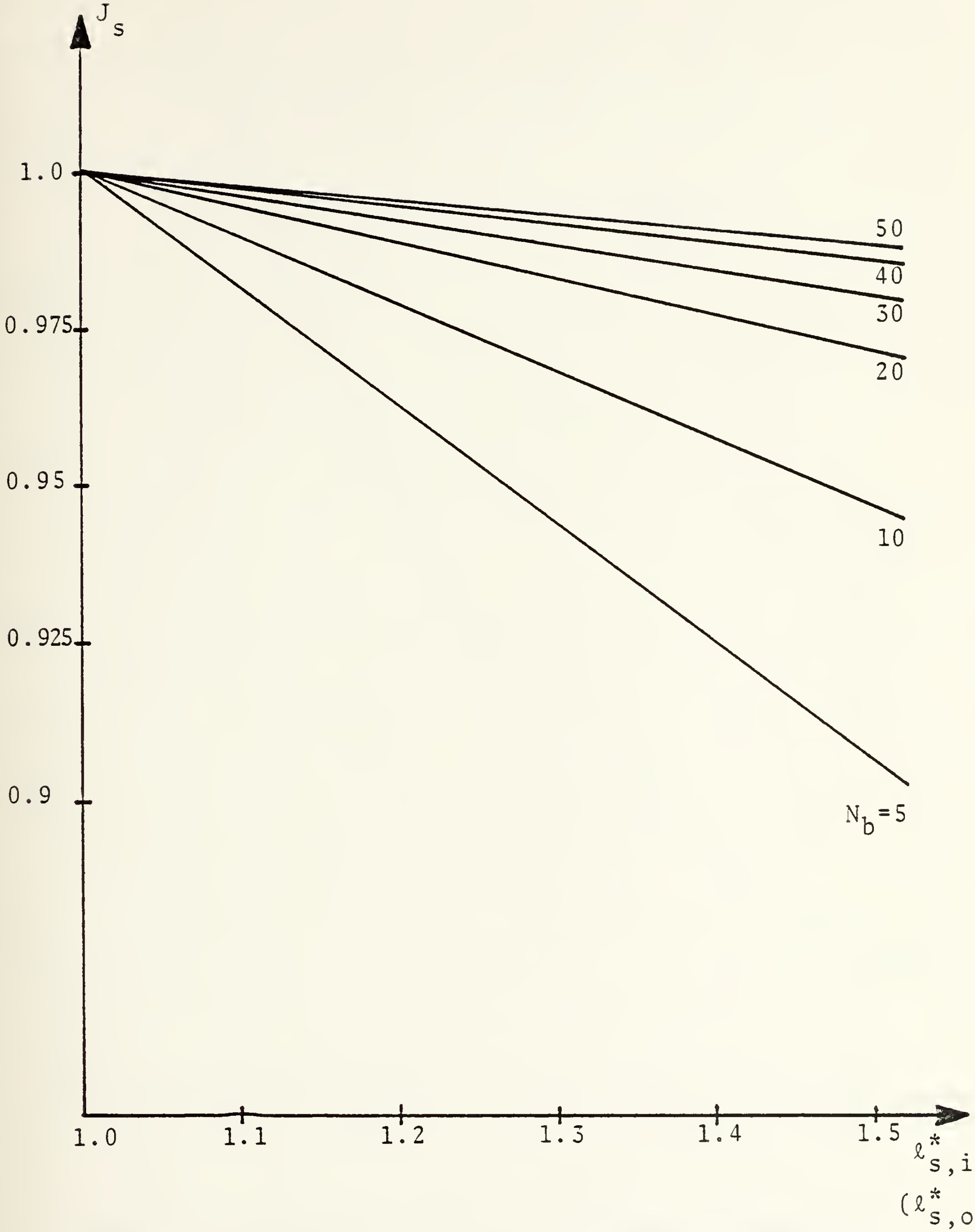

FIGURE 6 Correction Factor for Unequal Baffle Spacing, J_s vs $\ell^*_{s,i}$ $(=\ell^*_{s,o})$

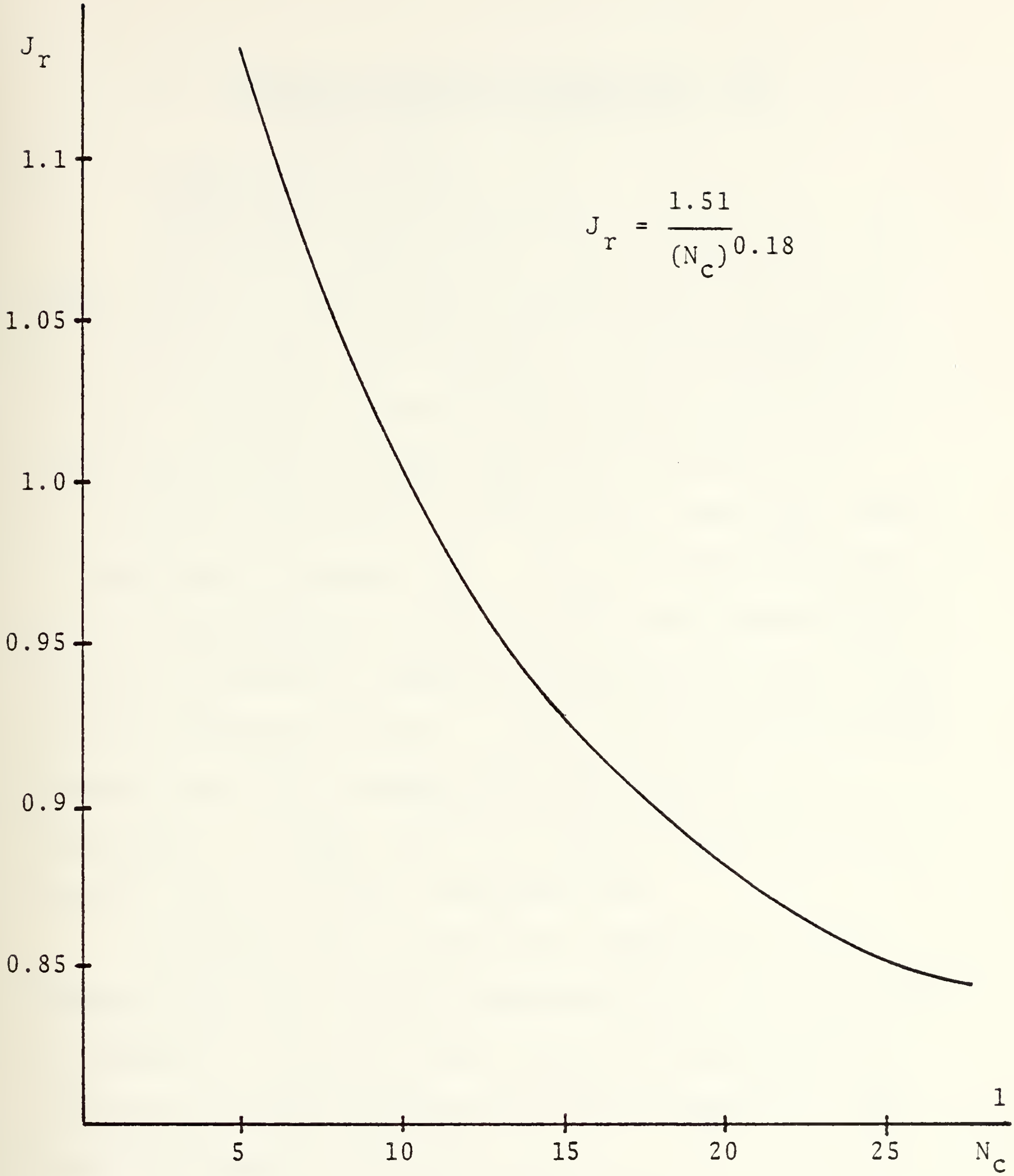

FIGURE 7 Correction Factor for Adverse Temperature Gradients, J_r vs N_c

II. CORRECTION FACTORS INFLUENCING THE HEAT TRANSFER COEFFICIENT

A. BUNDLE BYPASS FACTOR -- J_b

The bundle bypass factor, J_b, accounts for the effect of fluid flow between the shell and outer tubes of the tube bundle. This portion of the flow bypasses the main crossflow section of the tube bank and has a significant effect on heat transfer. Equations A-4, A-5, and A-18 are used to calculate J_b, where the shell-to-tube-bundle clearance $(D_i - D_{otl})$ has been approximated by equation (3). Equation A-18 was developed by Mueller (7) where for laminar/transition flow $C_{bh} = 1.35$ and for turbulent flow $C_{bh} = 1.25$. For purposes of this analysis only two regimes of Reynolds numbers are considered: $1 < Re_s < 10^3$ for laminar/transition flow and $10^3 < Re_s < 10^5$ for turbulent flow.

The non-linear regression results for J_b are presented in Table 4 and a representative curve is shown in Figure 8. As can be seen, J_b can be represented as a function of shell diameter D_i, tube diameter d_o, and pitch-to-diameter ratio P/d_o.

From Table 4, it can be readily seen that tube diameter has little effect on J_b. Over the range of d_o considered $(0.5<d_o<1.5)$, the change in J_b due to

increasing (or decreasing) d_o from 1.0 to 1.5 (or to 0.5) is less than 1%.

Figure 8 is applicable only for turbulent flow over square tube orientations. However, we may estimate J_b for other flow/orientation conditions easily from Table 4 and can estimate changes in J_b in the following fashion. If J_b is desired for rotated-square layouts in turbulent flow, we may form a ratio:

$$\frac{J_{b_r}}{J_{b_s}} = \frac{[C_o\ (P/d_o)^{a_2}\ (D_i)^{a_3}]r}{[C_o\ (P/d_o)^{a_2}\ (D_i)^{a_3}]s}$$

$$= \left(\frac{C_{o_r}}{C_{o_s}}\right)\ (P/d_o)^{a_{2_r} - a_{2_s}}\ (D_i)^{a_{3_r} - a_{3_s}} \tag{6}$$

This simple relation yields the result that rotated-square layouts, for $P/d_o = 1.5$, $D_i = 30$, result in a bundle bypass factor approximately 6% higher than square tube orientations.

Such insight into the intricacies of the Delaware Method can allow the designer to make reasonable "fine-tuning" corrections to a preliminary design without the need for costly (and sometimes cumbersome) computer models.

$$J_b = c_o\,(d_o)^{a_1}\,(P/d_o)^{a_2}\,(D_i)^{a_3}$$

R_{e_s}	Layout	c_o	a_1	a_2	a_3
$1 - 10^3$	Square	.335	-.0137	.5249	.1806
	Rotated-Square	.416	-.0119	.4358	.1493
	Triang.	.496	-.0099	.3503	.1194
$10^3 - 10^5$	Square	.369	-.0125	.4789	.1648
	Rotated-Square	.445	-.0108	.3976	.1362
	Triang.	.527	-.009	.3197	.1089

TABLE 4 Correlation Results for Baffle Configuration Factor, J_b

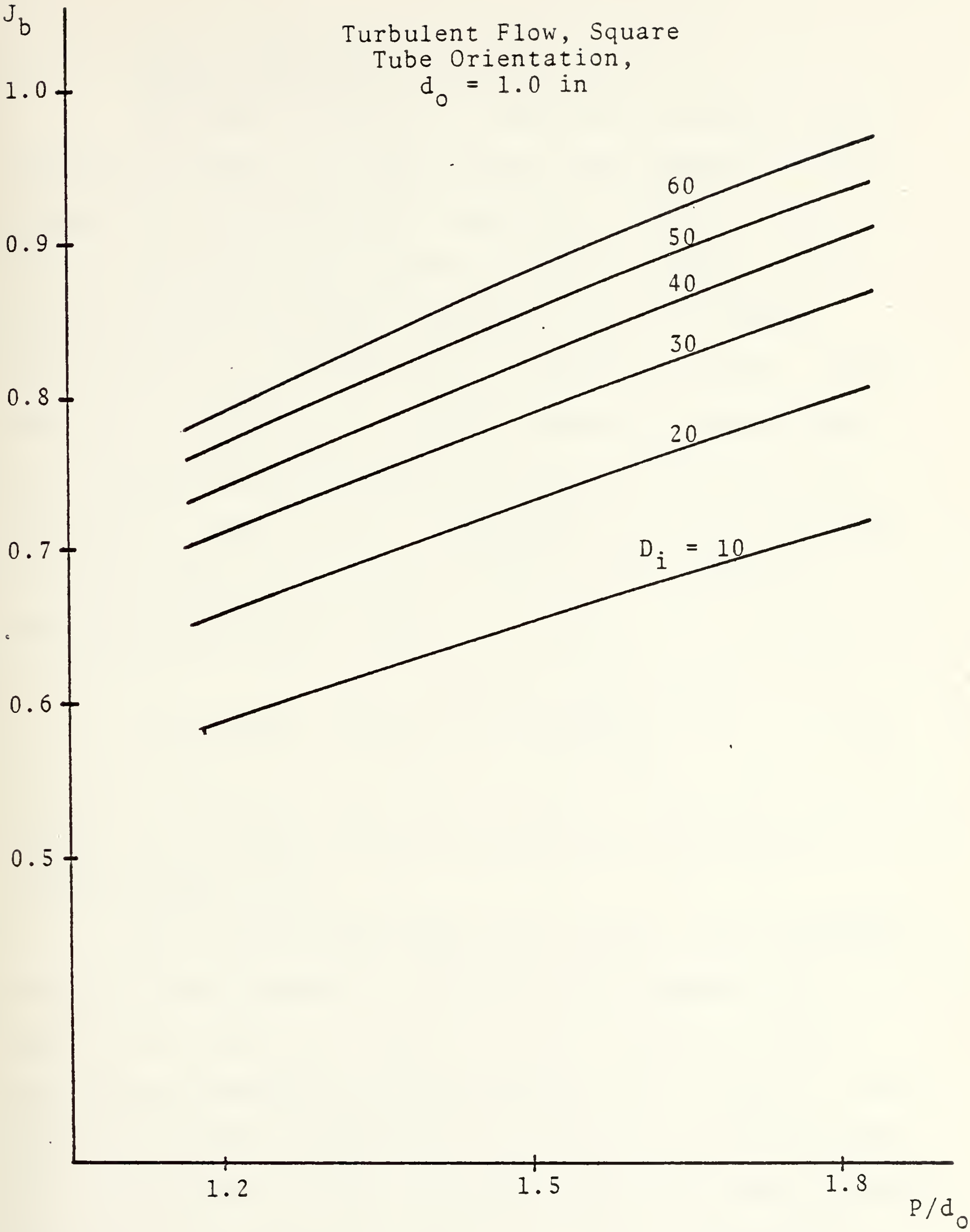

FIGURE 8 Bundle Bypass Factor J_b vs P/d_o

B. BAFFLE CONFIGURATION FACTOR -- J_c

Equations A-2 and A-16 represent the baffle configuration factor, J_c, which amounts for changes in heat transfer due to those tubes physically located in the baffle window and not subjected to full corssflow from the main stream of fluid. Equation A-16 is a linear approximation to the graph of J_c developed by Bell. Using equation (3) for $D_{ot\ell}$, J_c can be reasonably approximated as a product of shell diameter and baffle cut (or baffle cut ratio). This result is independent of flow condition and tube orientation. Regression analysis results in the following equation for J_c:

$$J_c = 0.492\ (\ell_c/D_i)^{-0.5467}\ (D_i)^{-0.0184} \qquad (7)$$

Figure 9 is a family of curves plotting ℓ_c/D_i vs J_c at various values of D_i.

As is easily seen from this figure, the dependence of J_c on shell diameter is minimal when compared with that of the baffle cut ratio. For the range of baffle cut ratios considered in this analysis ($0.2 < \ell_c/D_i < 0.4$), the heat transfer coefficient may vary from a 15% increase to a 25% decrease. Bell (1) states that for "well-designed" exchangers, J_c should be about 1.0, which corresponds to a value of ℓ_c/D_i of about 0.25.

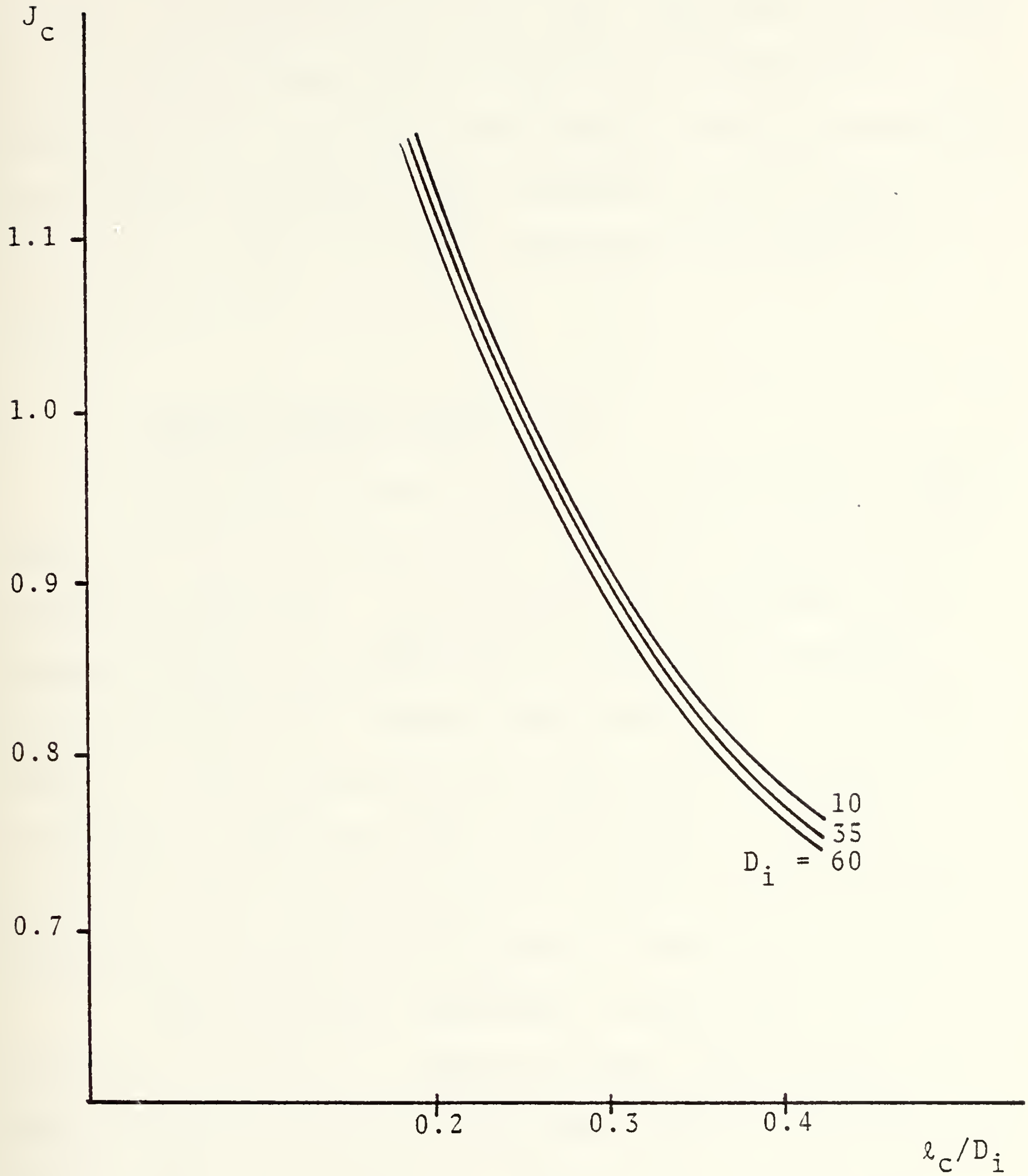

FIGURE 9 Baffle Configuration Factor J_c vs Baffle Cut Ratio ℓ_c/D_i

It is interesting to note that in the optimization routines of references (9) and (10), the baffle cut ratios for "optimal" design were 0.25 and 0.2, respectively. Admittedly, the objective functions for these optimizations were slightly different (heat transfer area and total tube length, resp.), but the similarity of results is significant.

C. BAFFLE LEAKAGE FACTOR -- J_ℓ

The baffle leakage factor, J_ℓ, is by far the most complex of all the factors affecting the overall heat transfer coefficient. It accounts for the effect of leakage through the baffle due to clearances between baffle and shell and between tube and baffle. In this regard, it is a function of all five basic exchanger parameters. Equations A-6, 7, 8, 15, 16, 17 must all be used in the calculation of J_ℓ, where some additional dependence is noted as a function of tube orientation.

The non-linear regression results for J_ℓ are presented in Table 5. Numerous graphs and families of curves can be generated using these results. However, for the sake of simplicity, Figures 10a, b, and c are represenative of the effect on J_ℓ of several parameter variations. Bell states that the value of J_ℓ should

$$J_\ell = c_o(d_o)^{a_1} (P/d_o)^{a_2} (\ell_c/D_i)^{a_3} (\ell_s/D_i)^{a_4} (D_i)^{a_5}$$

Layout	c_o	a_1	a_2	a_3	a_4	a_5
Square	0.572	0.1296	0.7745	0.0975	0.2708	0.0718
Rotated-Square	0.613	0.1177	0.7136	0.0856	0.2339	0.0643
Triangular	0.656	0.1127	0.6679	0.0767	0.2051	0.0516

TABLE 5 Correlation Results for Baffle Leakage Factor, J_ℓ

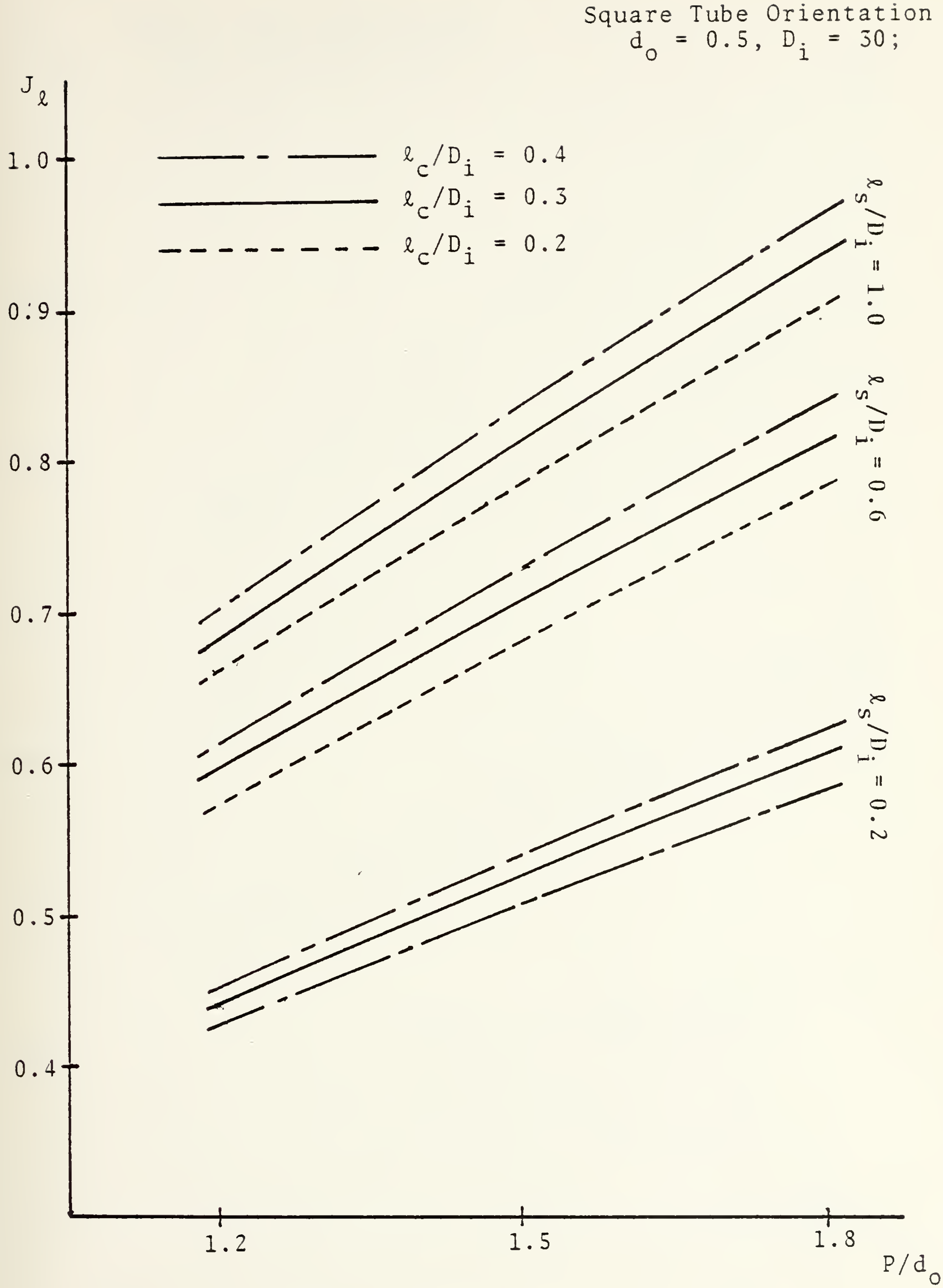

FIGURE 10a Baffle Leakage Factor J_ℓ vs P/d_o

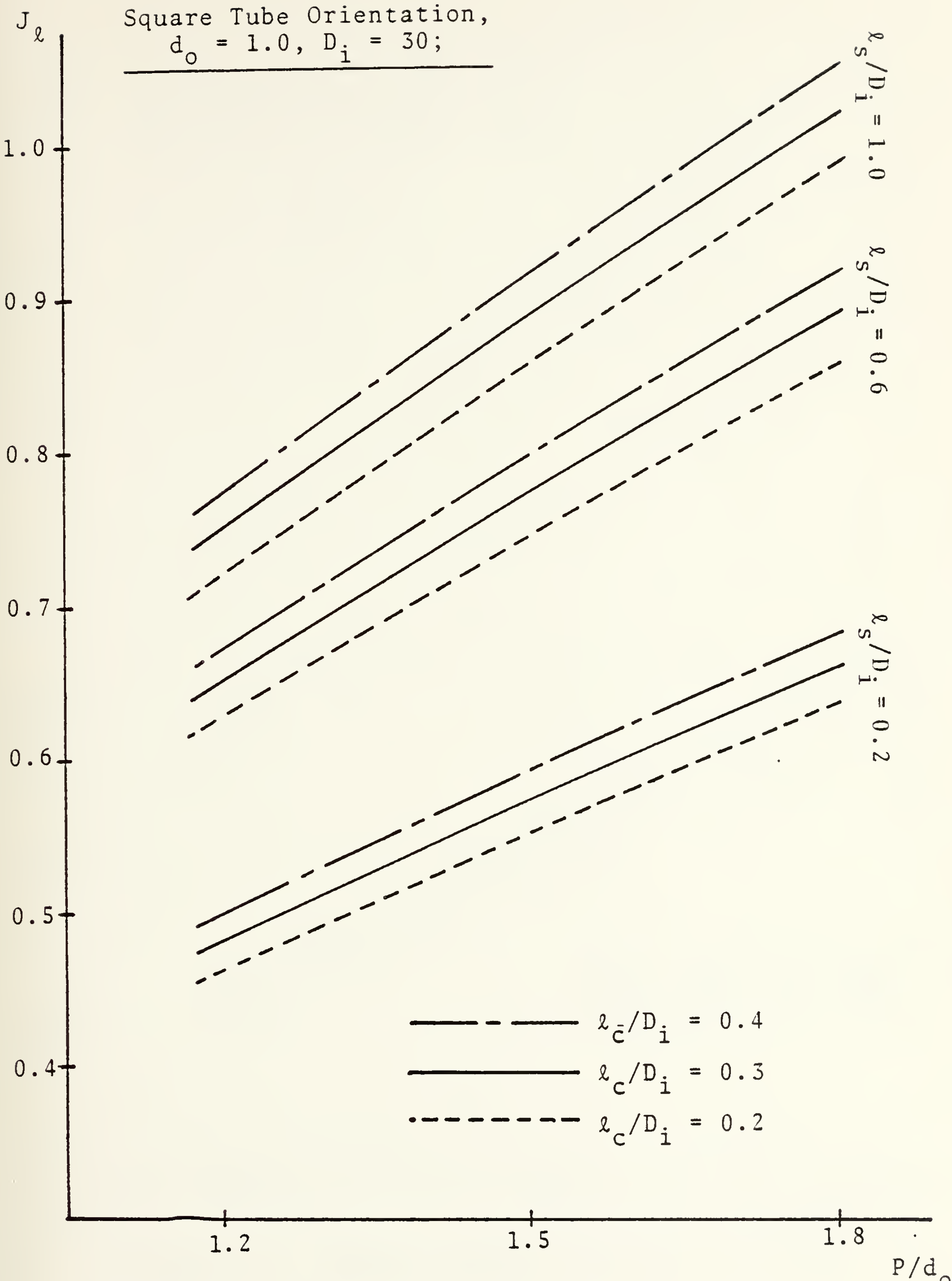

FIGURE 10b   Baffle Leakage Factor J_ℓ vs P/d_o

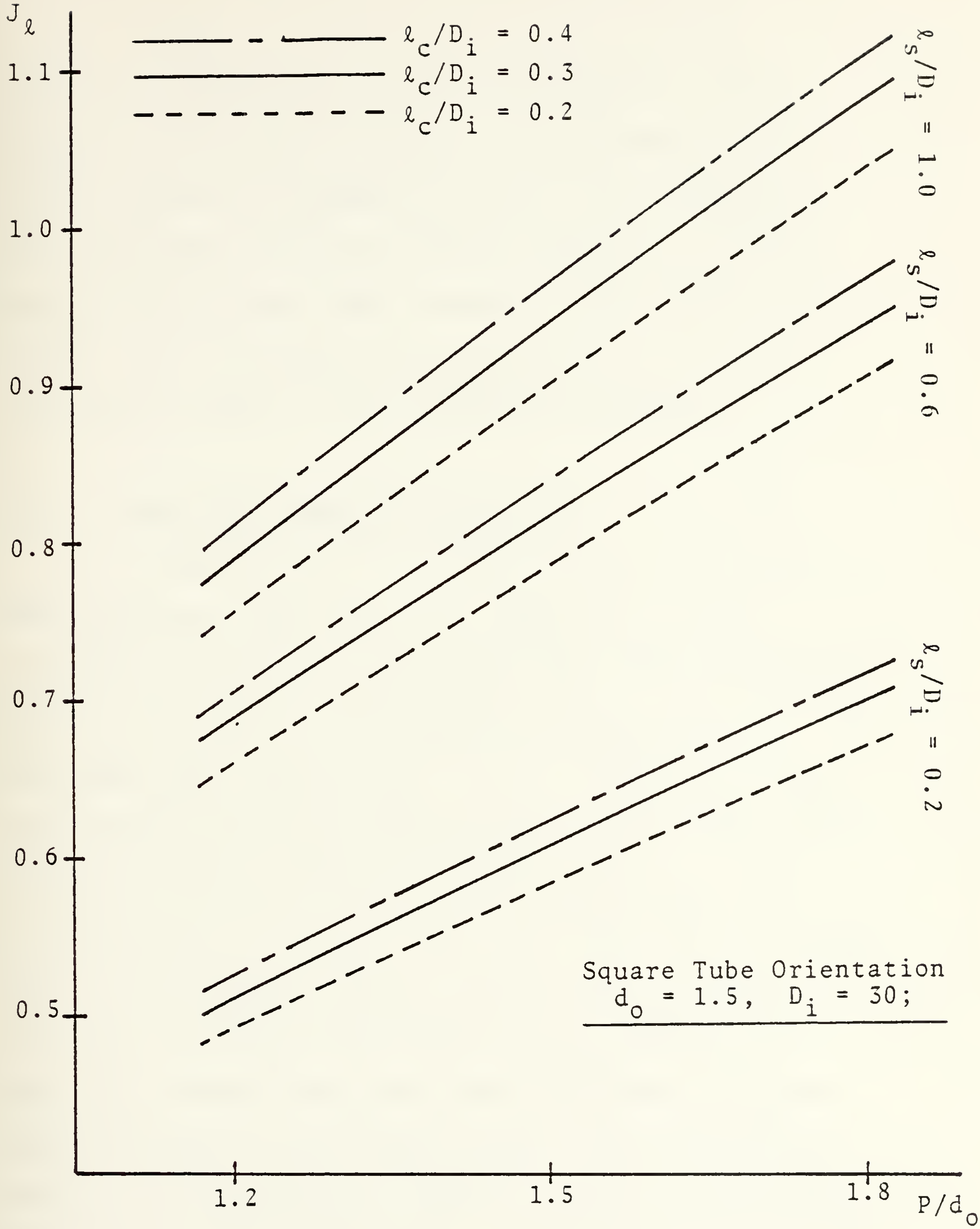

FIGURE 10c Baffle Leakage Factor J_ℓ vs P/d_o

be 0.7 -- 0.8 for well-designed exchangers. From Figure 10, one can easily read an appropriate value of the necessary parameter that will be a reasonable starting point for heat exchanger design. For other shell diameters and tube diameters, the relations of Table 5 may be suitably manipulated to arrive at reasonable values of the necessary parameters.

D. MULTIPLE CORRELATION RESULTS

To facilitate the overall prediction of the heat transfer coefficient as a function of those variables considered, the actual shell side coefficient, h_o, was calculated as a product of h_{ideal} and the aforementioned factors: J_b, J_c, J_ℓ. Colburn j-factor correlations of Table 1 were used for the various flow regimes as were correlations for N_t and $\delta_{st\ell}$. The fluid properties and mass flow rate terms were factored out of the equation and only those terms involving geometric parameters were used for the overall correlation. These terms were then correlated using the aforementioned Fortran subroutines. The correlation results are presented in Table 6 for the various flow regimes and tube orientations. It should be noted that all input dimensions for the exchanger parameters are

in inches and that the correction factors inherent in these equations have been accounted for in the correlation constant. The resulting units for h_o are those typically expected of the English system, Btu/HR-FT^2-^oF. The units for fluid properties are as listed in the nomenclature.

Table 6 is a "busy" listing and many graphical representations can be drawn plotting the heat transfer coefficient h_o against the various parameters. That will not be done here but some aspects of Table 6 are noteworthy.

Most exchangers are designed for operation in turbulent flow and for this regime it can be seen that h_o is nearly inversely proportional to shell diameter, the exponent a_5 being close to -1.0. This is a striking result, in that for desired increases in h_o, changes in shell diameter maybe the most rapid means of attaining the desired value.

The dependence of h_o on baffle cut ratio, ℓ_c/D_i, is independent of flow but dependent on tube orientation, and h_o varies nearly as the square-root of ℓ_c/D_i. Pitch-to-diameter ratio, P/d_o, has little effect on square tube orientations, but can cause significant changes in triangular and rotated square patterns. The dependence of h_o on tube diameter and

baffle spacing ratio is straightforward and needs no further explanation.

From Table 6 it is quite easy to predict the heat transfer coefficient given the exchanger geometric parameters and fluid properties. Only a quick Reynolds number calculation is necessary beforehand to determine the applicable flow regime. Changes in h_o are predicted simply by calculating the ratio of the parameter varied raised to the appropriate exponent. This is quickly accomplished if only one parameter is varied at a given time. For large changes one must be cautious that the flow regime remains as desired, i.e., turbulent or laminar/transition.

$$\frac{h_o}{K_1} = W_s \cdot \left(\frac{W_s}{\mu_s}\right)^{x_o} \cdot c_o \cdot (d_o)^{x_1} (P/d_o)^{x_2} (\ell_c/D_i)^{x_3} (\ell_s/D_i)^{x_4} (D_i)^{x_5}$$

$$K_1 = c_s (P_{rs})^{-2/3} \left(\frac{\mu_s}{\mu_{s,w}}\right)^{0.14}$$

R_{e_s}		c_o	x_o	x_1	x_2	x_3	x_4	x_5
	Square	6.3485	-.598	-.4672	-.1906	-.4492	-.1312	-.5432
$1 - 10^3$	Rotated Square	13.0147	-.6282	-.5074	-.5935	-.4611	-.1379	-.5391
	Triangular	14.3773	-.6114	-.4918	-.6601	-.47	-.1836	-.6282
	Square	4.0704	-.3532	-.2122	+.0152	-.4492	-.376	-1.0322
$10^3 - 10^5$	Rotated Square	6.9037	-.3976	-.2664	-.1154	-.4611	-.3685	-1.0077
	Triangular	7.319	-.3921	-.2623	-.3107	-.47	-.4028	-1.0792

TABLE 6 Correlation Results for Overall Shell Side Heat Transfer Coefficient, h_o

III. CORRECTIONS AFFECTING PRESSURE DROP

A. BAFFLE LEAKAGE FACTOR -- R_ℓ

The pressure drop correction factor for baffle leakage, R_ℓ, accounts for pressure drop changes in much the same fashion that J_ℓ accounts for changes in heat transfer. It relates the leakage through the baffle due to tube-to-baffle and baffle-to-shell clearances to the geometric parameters of the heat exchanger. Equations A-2, 4, 6, 7, 8, 14, 15, 20 and 21 are all used to calculate R_ℓ. Dependence on tube orientation is accounted for in equations A-4 and A-6 by the use of the correlations for N_t in Equations (1) and (2) and the tube pitch relations of Table 3.

The non-linear correlation results are presented in Table 7 and a representative graph as Figure 11. Figures 10 and 11 show a striking resemblance of form, which is to be expected. One can logically assume that an increase in heat transfer coefficient due to less leakage through the baffle will also result in increased pressure drops.

$$R_\ell = a_o (d_o)^{a_1} (P/d_o)^{a_2} (\ell_c/D_i)^{a_3} (\ell_s/D_i)^{a_4} (D_i)^{a_5}$$

Layout	a_o	a_1	a_2	a_3	a_4	a_5
Square	.2985	.2217	1.315	.1754	.4674	.1584
Rotated Square	.328	.1798	1.147	.1475	.3954	.157
Triangular	.3702	.1682	1.0696	.1318	.3496	.1365

TABLE 7 Correlation Results for Baffle Leakage Factor R_ℓ

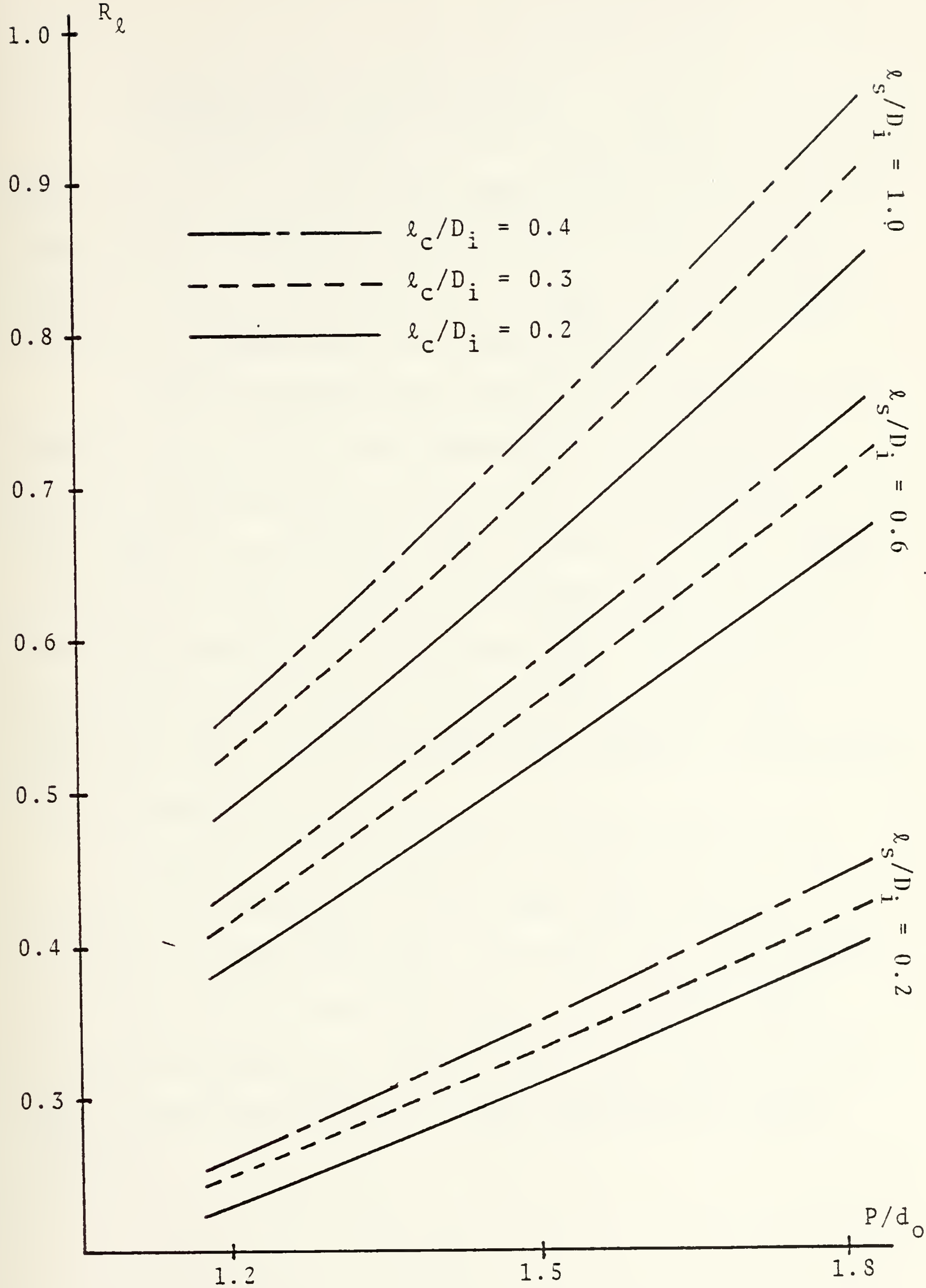

FIGURE 11 Baffle Leakage Factor R_ℓ vs P/d_o

B. BUNDLE BYPASS FACTOR -- R_b

The bundle bypass factor, R_b, accounts for pressure drop corrections in the same manner that J_b accounts for heat transfer changes. From Equation A-22, it can be seen to relate that correction to F_{sbp}, the fractional crossflow area available for bundle bypass.

Table 8 presents the correlation results for R_b. Similar to J_b is the weak dependence on tube diameter and the strong dependence on pitch-to-diameter ratio. This comes as no surprise since increases in P/d_o "open up" area for flow through the crossflow bank, thereby decreasing the fraction of bypass area. The increase in R_b with increasing D_i is less than that of P/d_o, since the shell-to-outer-tube-limit clearance (Equation 3) also increases with D_i.

Figure 12 is a graphical representation of R_b vs. P/d_o at various D_i, in the same manner as Figure 8. It should be noted that over the range of d_o considered ($0.5 < d_o < 1.5$), the value of R_b will decrease about 5% with increasing d_o, a much larger percentage decrease than can be predicted for J_b (and subsequently, heat transfer).

$$R_b = a_o (d_o)^{a_1} (P/d_o)^{a_2} (D_i)^{a_3}$$

R_{e_s}	Layout	a_o	a_1	a_2	a_3
$1 - 10^3$	Square	.0277	-.0449	1.7242	.5932
	Rotated Square	.0542	-.0389	1.431	.4903
	Triangular	.0999	-.0324	1.1508	.392
$10^3 - 10^5$	Square	.0524	-.0369	1.4177	.4878
	Rotated Square	.0909	-.032	1.177	.403
	Triangular	.1504	-.0267	.9462	.322

TABLE 8 Correlation Results for Bundle Bypass Factor, R_b

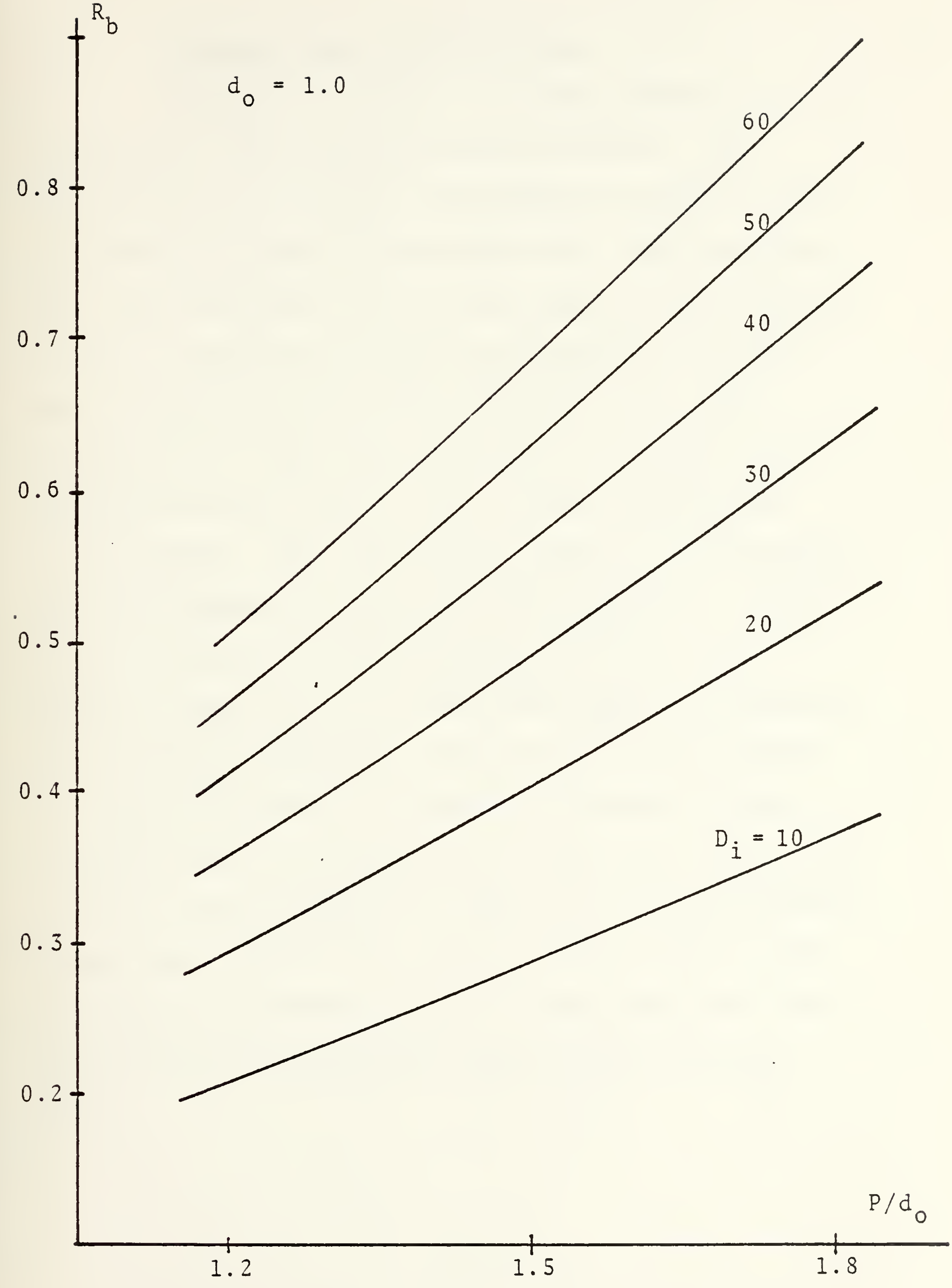

FIGURE 12 Bundle Bypass Factor, R_b vs P/d_o

C. CROSSFLOW AREA PRESSURE DROP

Equation A-23 gives the ideal pressure drop for flow across the tube bank between baffles. When multiplied by R_b and R_ℓ, the effects of bundle bypass and baffle leakage are accounted for. This quantity has been correlated in the same manner as the previous values. The friction factor correlations of Table 2 were used along with other corrections for tube orientation. Table 9 is the result of these overall correlations for the two flow regimes and various orientations. Note that the exponent x_6 of the basic equation depends on flow and orientation as a result of the friction factor correlation. Hence, the pressure drop can not be expressed <u>only</u> as a function of exchanger parameters. From Table 9 it is obvious that <u>all</u> the geometric parameters inversely affect pressure drop, a result that may have been intuitively obvious, but the extent of which can now be reasonably quantified. Essentially, the increase in any of the five basic parameters allows for more area for fluid flow with less restriction; hence, lower pressure drops.

$$N_b \cdot \frac{\Delta P_{b,i} \cdot R_b \cdot R_\ell}{\frac{W_s^2}{g_c \rho_s} \cdot \left(\frac{\mu_{s,w}}{\mu_s}\right)^{0.14}} = a_o \, (d_o)^{a_1} \, (P/d_o)^{a_2} \, (\ell_c/D_i)^{a_3} \, (\ell_s/D_i)^{a_4} \, (D_i)^{a_5} \left(\frac{W_s}{\mu_s}\right)^{a_6} L$$

R_{e_s}	Tube Pattern	a_o	a_1	a_2	a_3	a_4	a_5	a_6
$1 - 10^3$	Square	966.65	-1.6335	-4.3402	-1.3712	-1.6797	-1.4662	-.8528
	Rotated Square	257.58	-1.5548	-4.8924	-1.399	-1.8584	-1.8291	-.7462
	Triangular	534.25	-1.5573	-5.631	-1.4147	-1.9035	-1.9889	-.747
$10^3 - 10^5$	Square	115.05	-.80997	-3.3524	-1.3712	-2.466	-3.0922	-.0664
	Rotated Square	36.56	-.9043	-2.9907	-1.399	-2.477	-3.1381	-.1276
	Triangular	51.27	-.8886	-3.7658	-1.4147	-2.5391	-3.3355	-.1114

TABLE 9 Correlation Results for Crossflow Area Pressure Drop

D. WINDOW AREA PRESSURE DROP

Equation A-23 gives the ideal pressure drop for the baffle window section of the heat exchanger. When multiplied by R_{ℓ}, the effect of baffle leakage is taken into account. Correlation results are presented in Table 10 for differeing tube orientations. Unlike crossflow pressure drop, this quantity is independent of flow regime.

These results are very similar to the crossflow pressure drops in that pressure drop is inversely proportional to <u>all</u> variables. However, in the window area the relative importance of the parameters is slightly different. For the window area, shell diameter is the predominant influencing factor instead of pitch-to-diameter ratio. The relative influence of baffle cut and a baffle spacing ratios is nearly the same for both area pressure drops. Tube diameter impact is relatively the smallest for the turbulent crossflow area pressure drop.

$$N_b \frac{\Delta P_{w,i} \cdot R_\ell}{W_s^2/g_c\ \rho_s} = L \cdot a_o (d_o)^{a_1} (P/d_o)^{a_2} (\ell_c/D_i)^{a_3} (\ell_s/D_i)^{a_4} (D_i)^{a_5}$$

Tube Pattern	a_o	a_1	a_2	a_3	a_4	a_5
Square	4276.92	-.3323	-2.0127	-0.57	-1.5326	-4.1377
Rotated Square	4574.76	-.4397	-2.3711	-0.5284	-1.6046	-4.106
Triangular	4695.6	-.4089	-2.7318	-0.5637	-1.6505	-4.1757

TABLE 10 Correlation Results for Window Area Pressure Drop

IV. PERFORMANCE AND SIZING OF HEAT EXCHANGERS

A. SENSITIVITY ANALYSIS OF HEAT TRANSFER PER UNIT PRESSURE DROP

For any given application, when determining the "optimal" size of a heat exchanger, some feel for the overall effect of parameter variations on heat exchanger performance is needed in order to judge the direction in which the design variables should be altered to arrive at a reasonable result. The performance of a heat exchanger, or the criterion against which an exchanger is to be considered optimal, can vary widely depending on the depth of the analysis that is being performed. In most practical applications the ultimate criterion is cost. In this analysis, cost will not be considered but a factor which can influence cost to some extent will be analyzed.

From the corrleation results for heat transfer coefficient, Table 6, and the basic heat balance:

$$Q = AU_o \, \Delta T_{\ell m} \tag{8}$$

consider the case where U_o is primarily dependent on h_o. Equation (8) then can be written as:

$$\frac{Q}{\Delta T_{\ell m}\ W_s K_1} = Ah_o$$

where K_1 is defined in Table 6. But $A = \pi d_o N_t L/12$ (ft^2), and the results from Equation (1) (or (2)) can be used for N_t to express A in terms of d_o, D_i, P/d_o. Define:

$$\Gamma_h \quad \text{as} \quad \frac{Q}{\Delta T_{\ell m}\ W_s K_1}$$

which yields:

$$\Gamma_h/L = \frac{\pi\ d_o\ N_t\ h_o}{12} \tag{9}$$

This quantity is a non-dimensional expression for heat transfer per unit length of the heat exchanger. From the correlation results for crossflow and window area pressure drops, (Tables 9 and 10), we may form, similarly:

$$\Gamma_p/L = \frac{N_b}{W_s{}^2/g_c\ \rho_s} \ (\Delta P_{b,i} + \Delta P_{w,i})/L \tag{10}$$

This is a simplified expression for the total shell-side pressure drop per unit length of heat exchanger. Then

Γ_h/Γ_p can be expressed as a quotient of those correlations already derived. It can be seen from all the correlation results that Γ_h/Γ_p is not only dependent on the geometry of the exchanger but flow rate also, specifically, W_s/μ_s. For this analysis, we will consider only turbulent flow across square-oriented tube bundles. The applicable correlation results were selected, the ratio Γ_h/Γ_p formed and that ratio was graphed as a function of the exchanger parameters. It should be noted that a Reynolds number of 10^4 was used, resulting in a value of $W_s/\mu_s = 2.026 \times 10^5$ at the mid-range of the exchanger geometry variables ($d_o = 1.0$, $P/d_o = 1.5$, $\ell_s/D_i = .6$, $D_i = 35$). Figures 13, 14, 15, 16 and 17 are various graphs of Γ_h/Γ_p. From Figures 13-17 it is obvious that shell diameter D_i is the most influential parameter affecting heat exchanger performance. Figure 13 graphically illustrates this influence for several values of baffle spacing ratio, ℓ_s/D_i. This is not to say that we should always optimize an exchanger at large values of D_i. Although Γ_h/Γ_p increases, this graph does not allow for any constraints to be considered, e.g. maximum shell-side pressure drop. However, we may conclude that where large amounts of heat are to be transferred with low shell-side pressure drops as a requirement, "large" shell diameters will be required.

Figure 14 illustrates the influence of baffle spacing on Γ_h/Γ_p at several values of D_i. This parameter also favorably affects the heat exchanger performance but certainly not to the extent of shell diameter. Again, the realization of the absence of a pressure drop constraint must be accounted for.

Figure 15 illustrates the relationship between Γ_h/Γ_p and tube diameter. This is the only parameter (of those considered) which adversely affects Γ_h/Γ_p. The most basic explanation for this effect is that increases in tube diameter will more quickly decrease heat transfer than they will pressure drop.

Figure 16 and 17 relate the effects of baffle cut ratio, ℓ_c/D_i and pitch-to-diameter ratio, P/d_o, to Γ_h/Γ_p. It is obvious that at the conditions analyzed (turbulent flow, square tube orientation), neither parameter has any significant effect on heat exchanger performance.

The five figures shown can be of assistance when determining exchanger size for a given "job". The qualitative effect (or lack thereof) of the five parameters will help guard against "false starts" in any iterative sizing scheme.

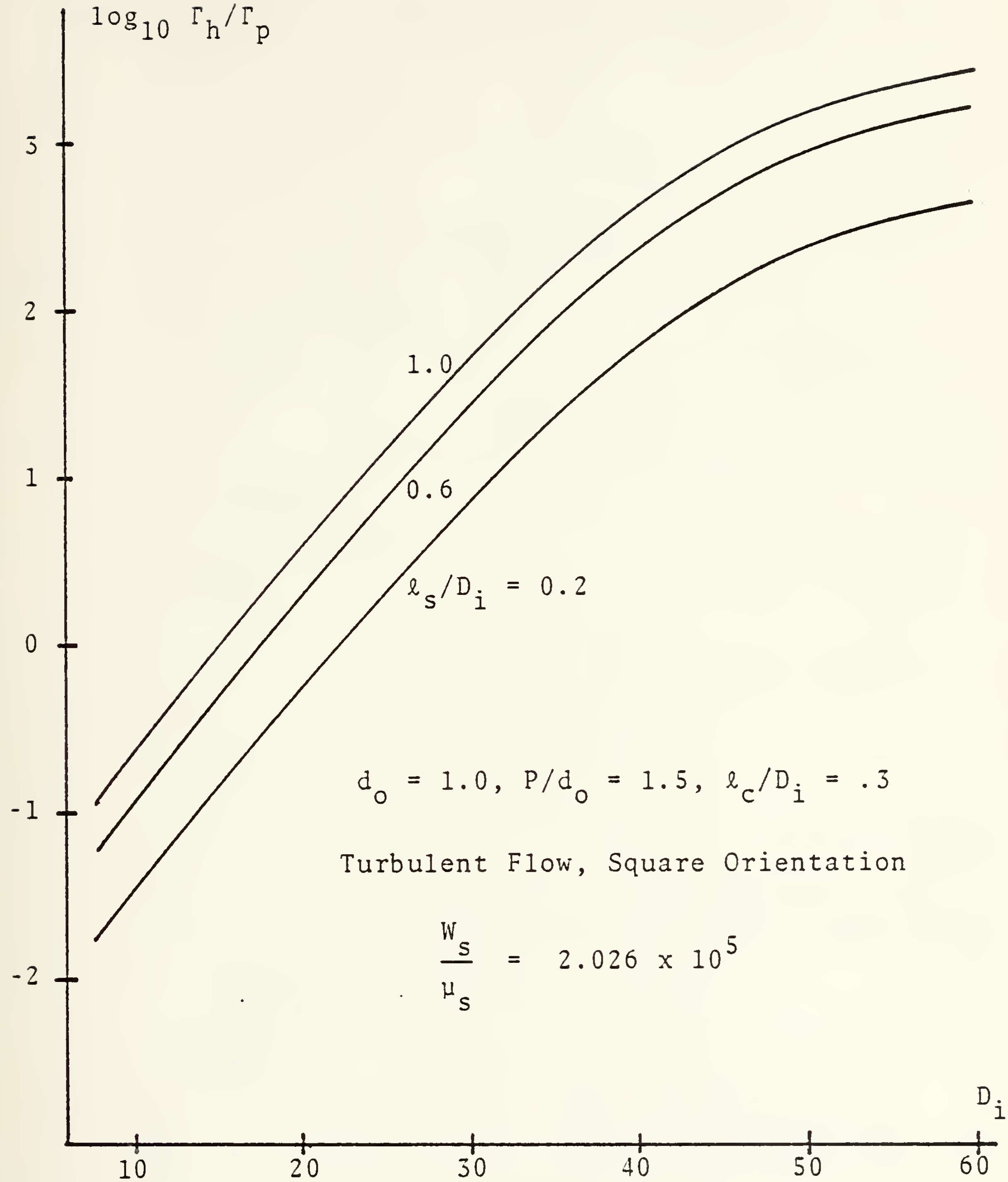

FIGURE 13 Γ_h/Γ_p vs D_i

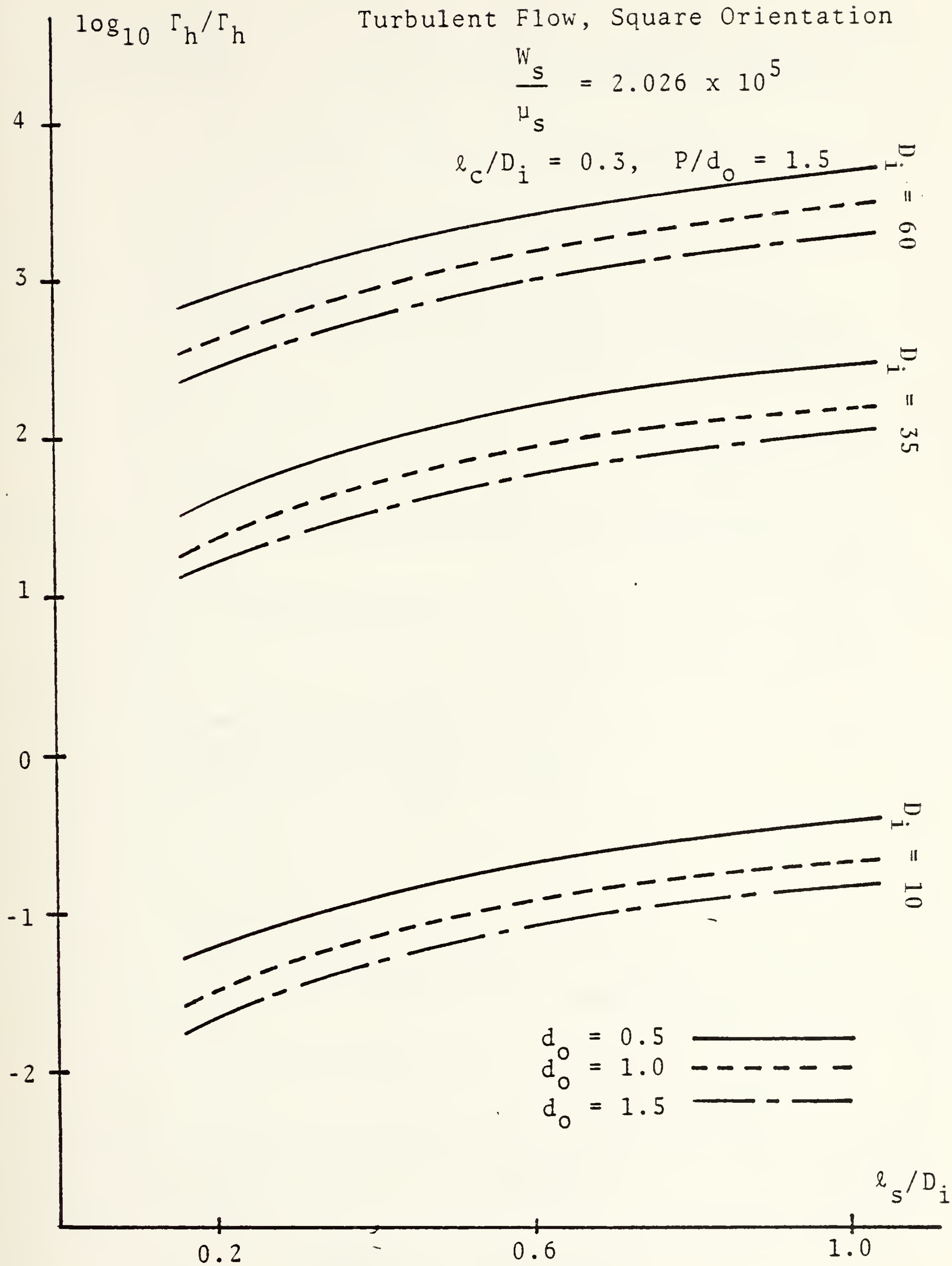

FIGURE 14 Γ_h/Γ_p vs ℓ_s/D_i

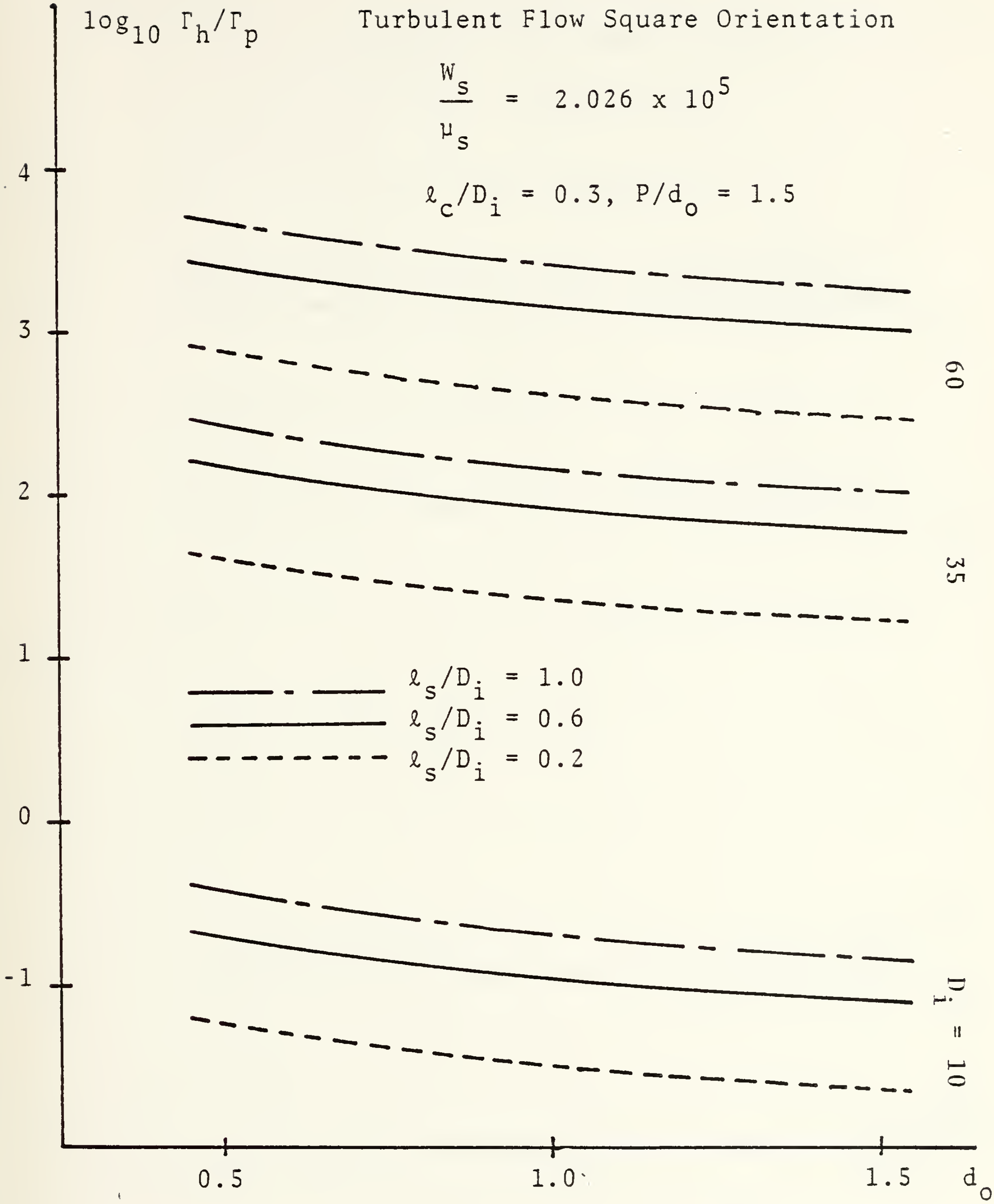

FIGURE 15 Γ_h/Γ_p vs d_o

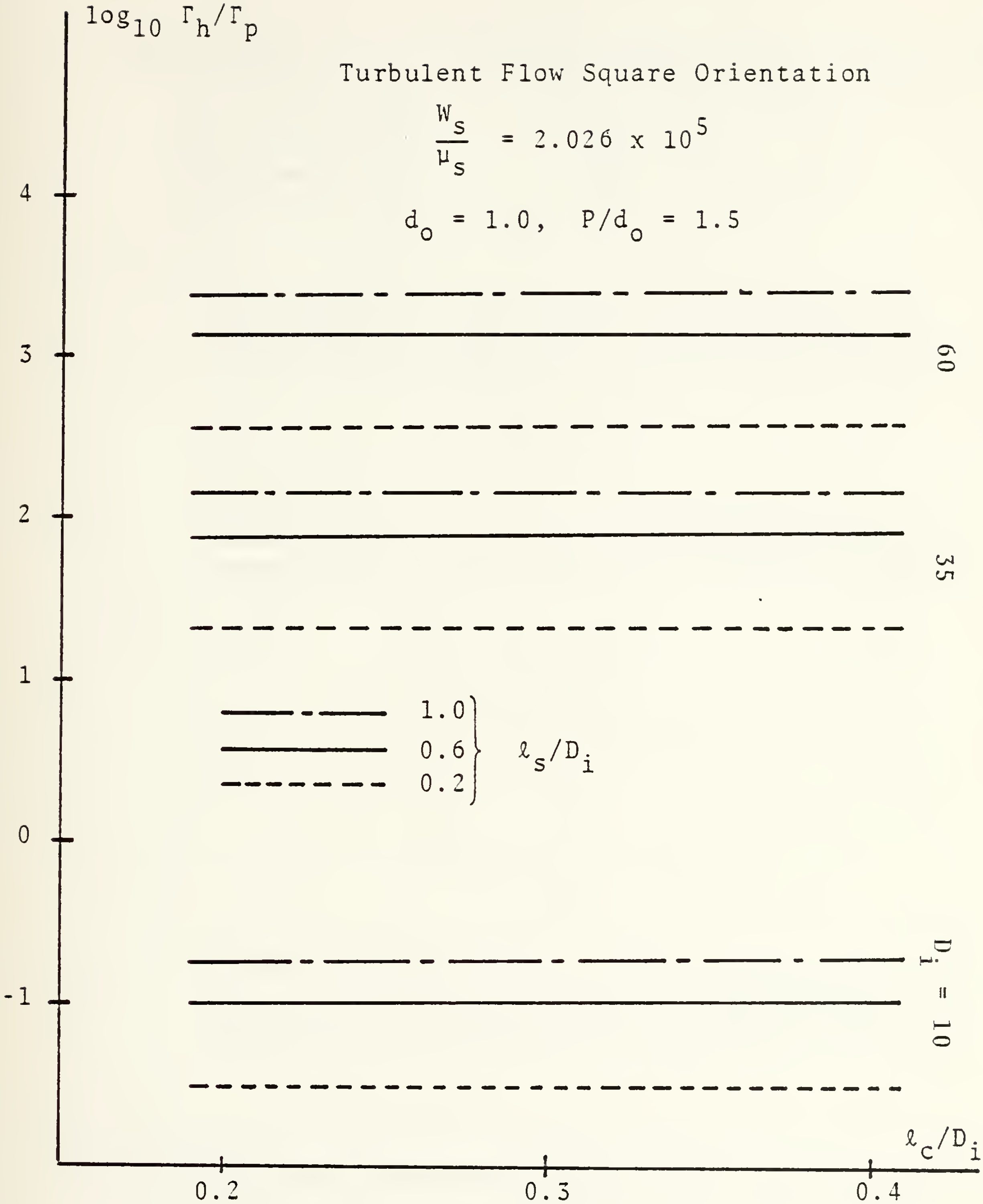

FIGURE 16 Γ_h/Γ_p vs ℓ_c/D_i

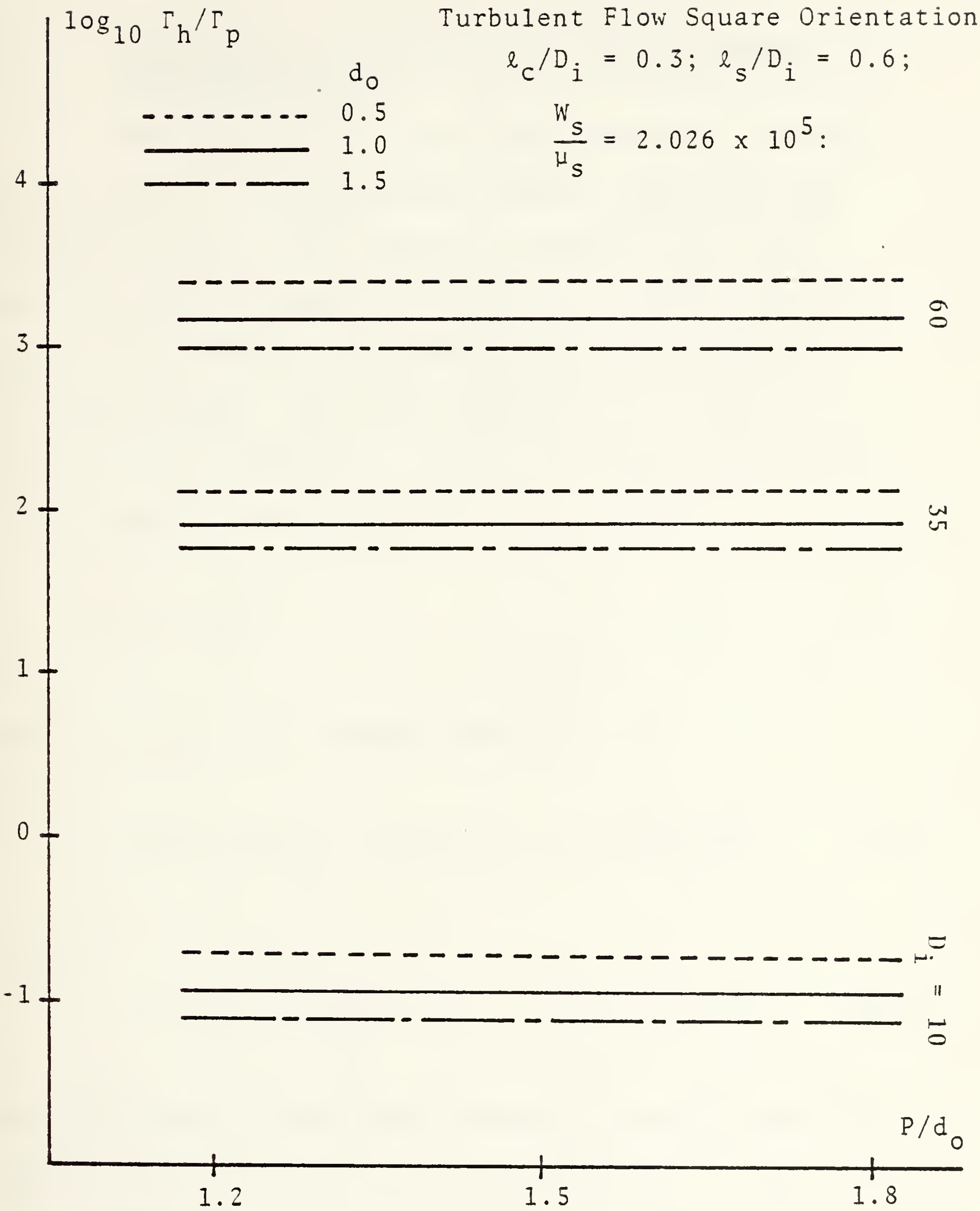

FIGURE 17 Γ_h/Γ_p vs P/d_o

B. PROPOSED SIZING ROUTINE FOR CASE OF SHELL-SIDE PROPERTIES ONLY

For the case where the shell-side heat transfer coefficient is the controlling factor (the tube side coefficient has little impact on overall U_o), it is desirable to determine the exchanger geometry for a given "job": total Q transferred; ΔP_s specified; W_s, ΔT_s (shell-side), and fluid properties all given. We may desire to "optimize" the heat exchanger on minimum volume where volume is simply expressed as:

$$V = \frac{\pi D_i^2}{4} L$$

From the basic heat balance equation,

$$Q = AU_o \Delta T_{\ell m}, \quad U_o \simeq h_o, \quad A = \frac{\pi d_o N_t L}{12} \tag{11}$$

yields

$$Q = \Delta T_{\ell m} \frac{\pi d_o N_t L}{12} h_o \tag{12}$$

With knowledge of the fluid properties we may form the quantity Γ_h:

$$\Gamma_h = \frac{Q}{\Delta T_{\ell m} K_1 W_s} \tag{13}$$

where K_1 is specified in Table 6, correlation results for shell-side coefficient. Then

$$\Gamma_h/L = \frac{\pi\ d_o\ N_t\ L}{12}\ h_o \tag{14}$$

We must now begin to specify the geometry of the exchanger. First, pick d_o, P/d_o, D_i as the beginning points. From equation A-12 for Reynolds number:

$$\begin{aligned} R_{e_s} &= \frac{12 d_o\ W_s}{\mu_s\ S_m} \\ &= \frac{W_s}{\mu_s}\ c_o\ (d_o)^{a_1}\ (P/d_o)^{a_2}\ (\ell_s/D_i)^{a_3}\ (D_i)^{a_4} \end{aligned} \tag{15}$$

where

$c_o = 62.224$, $a_1 = 1.037$, $a_2 = -\ 1.915$,

$a_3 = 1.0$, $a_4 = -\ 1.933$

we may either determine ℓ_s/D_i (if we desire to operate at a certain R_{e_s}) or pick ℓ_s/D_i and determine the flow regime (laminar/transition or turbulent).

Once this condition has been finalized, the proper correlation for h_o is selected from Table 6,

knowing the selected tube orientation. The last parameter to be determined is ℓ_c/D_i. As Bell has stated, for "well-designed" exchangers, J_c should be about 1.0, which, from Figure 6, yields a value of ℓ_c/D_i of about 0.25. The initial value of h_o may now be calculated from the correlation results of Table 6 and exchanger length L determined from Equation 10, using the proper N_t correlation for tube orientation. Volume may then be easily calculated.

Pressure drop calculations can be made from the correlation results of Tables 10 and 11, knowing the exchanger length L. This must then be checked against the allowed ΔP_s. If $\Delta P_{s_{calc}} < \Delta P_{s_{allowed}}$, we may decrease the size of the exchanger to utilize more of the allowed ΔP_s. This is most easily accomplished by decreasing D_i and recalculating h_o, L, ΔP_s and V, to arrive at some minimum volume.

If $\Delta P_{s_{calc}} > \Delta P_{s_{allowed}}$, the procedure is reversed, i.e., increase D_i and recalculate the necessary quantities until a convergence within some desired bound is obtained. As in the case in any sizing procedure, some notes of caution and guidelines are in order. When increasing shell diameter (or any of the other parameters), caution must be taken that the

flow regime remains as desired. It is also possible to "fine tune" the exchanger by altering the other geometric values. If the difference $\Delta P_{s_{calc}} - \Delta P_{s_{allowed}}$ is small, we may desire to change the baffle cut or baffle spacing ratios. Small changes in these parameters will also result in changes to the shell side pressure drop and heat transfer coefficient, the effect of which can be examined by the exponents of the applicable correlation result. We may also use Bell's insight into the heat transfer corrections to assure that the heat exchanger is reasonably well designed. For the heat transfer correction factors J_b, J_c, J_ℓ, Bell gives the following ranges as good guidelines:

$$J_c \approx 1.0$$

$$0.7 < J_b < 0.9$$

$$0.7 < J_\ell < 0.8$$

From Figure 9, 10, and 11, we can pick reasonable values of ℓ_c/D_i and ℓ_s/D_i as starting points for the exchanger geometry and, should changes be made, ensure that we remain in a normally expected range for those values. The use of those figures as aids to sizing should prevent haphazard variations and point to a reasonable solution

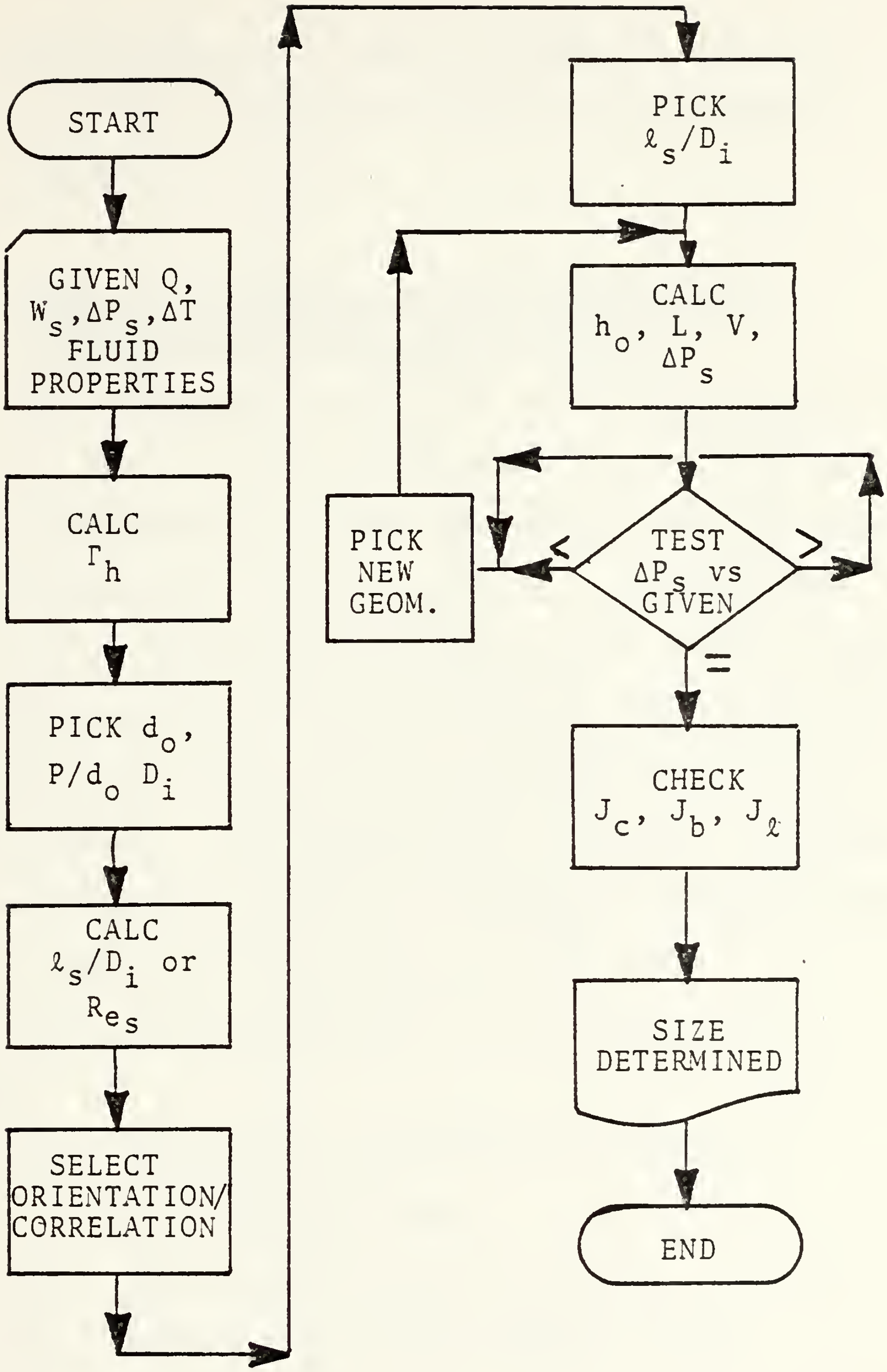

FIGURE 18 Simplified Logic Sequence for Proposed Sizing Routine

in an expedient manner. Figure 13 gives a simplified flow chart of the logical sequence for this proposed sizing routine.

C. EXAMPLE OF PROPOSED SIZING ROUTINE WITH COMPARISON TO THE DELAWARE METHOD

The preceding sections of this analysis have dealt with the actual results of the non-linear regression used to simplify the heat transfer coefficient and pressure drop calculations. In this section, a hypothetical example for determining exchanger size is given to show the actual mechanics of the proposed sizing routine and to compare those results with the calculations of the Delaware Method. This comparison is done for the case where only the shell-side heat transfer coefficient and pressure drop are of concern to the designer.

The "job" considered in this example is as follows:

1) shell-side mass flow rate of water:

   $W_s = 250{,}000$ lbm/hr

2) heat water from 50^oF to 90^oF

3) maximum shell-side pressure drop:

   $\Delta P_s \leq 8.0$ psi

The following fluid properties are assumed:

1) $c_c = 1.0$ btu/lbm - ^{o}F

2) $\mu_{s,w} = 1.65$ lbm/hr-ft (at an assumed $T_{wall} = 100^{o}F$)

3) $\mu_s = 2.445$ lbm/hr-ft (at $T_{ave} = 70^{o}F$)

4) $P_{r_s} = 7.05$

5) $\rho_s = 62.075$ lbm/ft^3

We desire to operate in the turbulent flow regime and must check the Reynolds number for our exchanger. Picking tube diameter $d_o = 0.75$ in, pitch-to-diameter ratio $P/d_o = 1.33$, baffle spacing ratio $\ell_s/D_i = 0.75$ and shell diameter $D_i = 25.0$ in, a check of Reynolds number using Equation (15) yields $Re_s = 7229$, which ensures turbulence. Using a square tube orientation, baffle cut ratio $\ell_c/D_i = 0.25$, we select the applicable correlation result from Table 6:

$$\frac{h_o}{K_1} = W_s \left(\frac{W_s}{\mu_s}\right)^{-.353} (4.07)(d_o)^{-.212} (P/d_o)^{.015}$$

$$(\ell_c/D_i)^{-.4492} \cdot (\ell_s/D_i)^{-.376} (D_i)^{-1.032}$$

where

$$K_1 = c_s \left(P_{r_s}\right)^{-2/3} \left(\frac{\mu_s}{\mu_{s,w}}\right)^{0.14}$$

Using the values given results in a heat transfer coefficient of:

$$h_o = 463.5 \text{ Btu/hr-ft}^3\text{-}^oF$$

From $Q = AU_o \, \Delta T_{\ell n} = Ah_o \Delta T_{\ell n}$, where

$$A = \frac{\pi \, d_o \, N_t \, L}{12} \quad \text{and} \quad N_t = 0.3559 \, \frac{D_i^{2.17526}}{d_o^{\,2}} \left(\frac{d_o}{P}\right)^2 ,$$

The length L of the heat exchanger is calculated:

$$L = 6.99 \text{ ft},$$

then volume

$$V = 23.83 \text{ ft}^3 .$$

Using the correlation results for crossflow and window area pressure drops from Tables 9 and 10 respectively, yields the total shell-side pressure drop:

$$\Delta P_s = .29 \text{ psi}$$

As a comparison, utilizing the Delaware Method (Reference 1), the following is presented:

	Proposed Method	Delaware Method
h_o (Btu/hr-ft^2-^oF)	463.5	454.8
L (ft)	6.99	7.05
V (ft^3)	23.83	24.03
ΔP_s (psi)	0.29	0.25

Although the results are quite close, we are far from "optimized" in using the allowed shell-side pressure drop. We may decrease shell diameter D_i to most easily accomplished this. For the next interation, pick D_i = 15.25 in. This "odd" size is picked only because Bell's tables in Reference (1) list all the applicable parameters for this size ($D_{ot\ell}$, N_t, etc.) and interpolation between those listed values would not result in a meaningful comparison.

A recalculation of the heat exchanger using this new value of D_i yields the following result:

	Proposed Method	Delaware Method
h_o	785.16	789.0
L	12.09	11.69
V	15.34	14.83
ΔP_s	3.62	3.61

These results are as agreeable as those of the first iteration, yet the exchanger may be further decreased in size. A third iteration, using D_i = 13.25 in yields:

	Proposed Method	Delaware Method
h_o	907.8	917.5
L	14.20	14.61
V	13.6	13.99
ΔP_s	7.53	7.27

These results show that we have come close to a preliminary size for the heat exchanger that meets the required "job". Some comments concerning the previous calculations are noteworthy.

In decreasing shell diameter in these iterations, the recalculation of h_o by the proposed method is accomplished simply by multiplying the previous value by the ratio of shell diameters raised to the applicable correlation exponent. Pressure drop calculations are estimated in much the same manner, except that the crossflow and window area terms must be done separately. The only "lengthy" calculation involves that of exchanger length, L.

For the sizing determination by the Delaware Method, no less than twenty-one (21) separate calculations and seven (7) graphical readings must be done for each iteration. For this proposed method only five (5) calculations were necessary: heat transfer coefficient (Table 6), overall length (Equation 12), pressure drops for crossflow and window sections (Tables 9 and 10), and total pressure drop (Equation A-25).

This quick, handy method is, in the opinion of this author, much more preferable to the original method for preliminary heat exchanger sizing and "back-of-the-envelope" calculations. It is realized that no simplified heat exahanger model can replace the more sophisticated computer optimization methods that have been and are being developed. However, in a relatively short time, the designer can achieve a realistic estimate of the heat exchanger performance and size, and can use these results as possible inputs to the more elaborate routines. The closer an initial estimate is to the actual optimum, the more time and money can be saved in the more sophisticated (and expensive) methods. Minimization of cost will almost always be a major goal.

APPENDIX A

Basic equations used for heat transfer coefficient and pressure drop calculations.

(1) $$N_c = \frac{D_i \left[1 - \frac{2\ell_c}{D_i}\right]}{P_p}$$

(2) $$F_c = \frac{1}{\pi}\left[\pi + 2\left(\frac{D_i - 2\ell_c}{D_{ot\ell}}\right) \sin\left(\cos^{-1}\frac{D_i - 2\ell_c}{D_{ot\ell}}\right) - 2\cos^{-1}\left(\frac{D_i - 2\ell_c}{D_{ot\ell}}\right)\right]$$

(3) $$N_{cw} = \frac{0.8\ \ell_c}{P_p}$$

(4) $$S_m = \ell_s\left[D_i - D_{ot\ell} + \left(\frac{D_{ot\ell} - d_o}{P_n}\right)(P - d_o)\right]$$

(5) $$F_{sbp} = [(D_i - D_{ot\ell})]\ \ell_s/S_m$$

(6) $$S_{tb} = \pi\ d_o\ \delta_{tb}\ N_t\ (1/2)\ (1 + F_c)$$

(7) $$\partial = 2\cos^{-1}\left(1 - \frac{2\ell_c}{D_i}\right)$$

(8) $$S_{sb} = \pi/2\ D_i\ \delta_{sb}\ [1 - \partial/2]$$

(9) $$S_{wg} = \frac{D_i^{\ 2}}{4}\left[\frac{\partial}{2} - \left(1 - \frac{2\ell_c}{D_i}\right)\sin \partial/2\right]$$

(10) $$S_{wt} = \frac{N_t}{8}\ (1 - F_c)\pi\ d_o^{\ 2}$$

(11) $$S_w = S_{wg} - S_{wt}$$

(12) $$R_{e_s} = \frac{d_o\ W_s}{\mu_s\ S_m} \cdot 12$$

(13) $$h_{ideal} = j_i\ c_s \left(\frac{W_s}{S_m}\right) (P_{rs})^{-2/3} \left(\frac{\mu_s}{\mu_{s,w}}\right)^{0.14}$$

(14) $$r_{\ell m} = \frac{S_{sb} + S_{tb}}{S_m}$$

(15) $$r_s = \frac{S_{sb}}{S_{sb} + S_{tb}}$$

(16) $$J_c = 0.55 + 0.72\ F_c$$

(17) $$J_\ell = 0.44\ (1 - r_s) + [1 - 0.44(1 - r_s)]e^{-2.2 r_{\ell m}}$$

(18) $$J_b = e^{[-C_{bh}\ F_{sbp}]}$$

(19) $$h_o = h_{ideal}\ J_c\ J_\ell\ J_b$$

(20) $$p = -\ 0.15\ (1 + r_s) + 0.8$$

(21) $$R_\ell = e^{[-1.33(1 + r_s) r_{\ell m}^p]}$$

(22) $$R_b = e^{[-C_{bp}\ F_{sbp}]}$$

(23) $$\Delta P_{b,i} = \frac{4\ f_i\ W_s^{\ 2}\ N_c}{2\ \rho_s\ g_c\ S_m^{\ 2}} \left(\frac{\mu_{s,w}}{\mu_s}\right)^{0.14}$$

$$\Delta P_{w,i} = \frac{W_s^{\,2}\,(2 + 0.6\, N_{cw})}{2\, g_c\, \rho_s\, S_m\, S_w} \tag{24}$$

$$\Delta P_s = [(N_b + 1)\, \Delta P_{b,i}\, R_b + N_b\, \Delta P_{w,i}]R_\ell \tag{25}$$

REFERENCES

(1) Bell, K.J., "Delaware Method for Shell Side Design", Heat Exchangers, Hemisphere Publishing Corporation, N.Y., N.Y.

(2) Tinker, T., "Shell Side Characteristics of Shell-and-Tube Heat Exchangers", Trans: ASME 80:36, 1958.

(3) Devore, A., "Try This Simplified Method for Rating Baffled Exchangers", Petroleum Refiner, Vol. 40, No. 5, May 1961, pp 221-233.

(4) Rohsenow, Warren, M., and Choi, Harry Yl, "Heat, Mass and Momentum Transfer, Prentice-Hall, Englewood Cliffs, N.J., 1961.

(5) Standards of Tubular Exchangers Manufacturers Association, 1968, 5th ed., TEMA, Inc., N.Y., N.Y.

(6) Scientific Subroutine Package (SSP) Library, Joint Computer Facility, MIT, Cambridge, MA.

(7) Private correspondence between Prof. W.M. Rohsenow and A. Mueller.

(8) Chemical Engineers Handbook, 5th ed., McGraw-Hill Book Co., N.Y., N.Y., 1973.

(9) Kaul, A.K., Mehta, S.I., and Sharma, G.K., "Computer Aided Design and Optimization of Shell-and-Tube Heat Exchangers", Journal of Thermal Engineering, Vol. 2, No. 2, 1981.

(10) Private communication between Professor Rohsenow, MIT and Professor Ralph Webb, Department of Mechanical Engineering, The Pennsylvania State University.

(11) Bell, K.J., "Exchanger Design Based on the Delaware Research Program", Petro/Chem Engineer, 32, pp C-26 - C-40C, October 1960.

199466

Thesis
E2323 Eden
c.1 The effect of design
parameters on shell-
side properties of
baffled shell-and-tube
heat exchangers.